

The final published version of this paper is available online at:  
[https://www.thelancet.com/journals/laninf/article/PIIS1473-3099\(17\)30421-8/fulltext](https://www.thelancet.com/journals/laninf/article/PIIS1473-3099(17)30421-8/fulltext)  
DOI: [https://doi.org/10.1016/S1473-3099\(17\)30421-8](https://doi.org/10.1016/S1473-3099(17)30421-8)

Title: Measles immunity gaps and the progress towards elimination: a model-based multi-country perspective.

Corresponding Author: Dr. Piero Poletti,

Corresponding Author's Institution: Fondazione Bruno Kessler

First Author: Filippo Trentini

Order of Authors: Filippo Trentini; Piero Poletti; Stefano Merler; Alessia Melegaro

Rights / License:

The terms and conditions for the reuse of this version of the manuscript are specified in the publishing policy. For all terms of use and more information see the publisher's website.

When citing, please refer to the published version.

## Title

# Measles immunity gaps and the progress towards elimination: a multi-country modelling analysis.

Filippo Trentini<sup>1,\*</sup>, Piero Poletti<sup>1,2,\*,#</sup>, Stefano Merler<sup>2</sup> and Alessia Melegaro<sup>1,3</sup>

<sup>1</sup> DONDENA Centre for Research on Social Dynamics, Bocconi University, Milan, Italy,

<sup>2</sup> Center for Information Technology, Bruno Kessler Foundation, Trento, Italy.

<sup>3</sup> Department of Policy Analysis and Public Management, Bocconi University, Milan

\* These authors contributed equally to this work.

# Corresponding author: poletti@fbk.eu

## Abstract

**Background.** Large measles epidemics still represent a persisting public health issue for both developing and developed countries. In order to progress towards measles elimination, it is crucial to identify population age segments that have not been adequately immunized across different socio-economic settings.

**Methods.** We developed a transmission model accounting for demographic processes and immunization activities implemented over the years to estimate current age-specific immunity profiles in nine countries with distinct demographic and vaccination histories. The model is calibrated on measles serological data and is used to assess the influence of local demographic conditions in shaping measles epidemiology and to indicate suitable adjustments of current vaccination strategies.

**Findings.** We found that, in low-income countries, the residual susceptibility is mostly concentrated in early childhood although Supplementary Immunization Activities have mitigated the effects of sub-optimal routine coverage. On the opposite, remarkable fractions of susceptibles were found across all ages in most industrialized countries, where routine first dose administration produced over 90% of the immunized individuals. Our analysis highlights that the consequences of past immunization programs, either beneficial or detrimental, persist longer in populations with an older age structure, due to a slower generational replacement.

**Interpretation.** Our results suggest the need for a change of current measles control strategies, based on local epidemiological and demographic conditions. Specifically, countries characterized by high fertility rates ought to optimize their routine immunization of young children. Catch-up campaigns are instead required in older populations, where susceptibility among adolescents and adults will otherwise sustain measles circulation.

## Introduction

Despite more than 20 years of immunization efforts, measles still represents one of the major causes of death among children under-five due to vaccine-preventable diseases [1]. The WHO Expanded Program on Immunization and Supplementary Immunization Activities, and the Measles Initiative have contributed in recent years to remarkably reduce the burden of disease in terms of incidence and mortality [2]. However, regular annual measles epidemics occur in several African countries, where infant mortality due to measles

infection is high [3]. Progress towards measles elimination is now questioned even in regions, like the Americas, where local elimination was temporarily achieved [4]. In particular, decreasing trends in coverage levels have been observed in Europe and US as a consequence of the emergence of anti-vaccination movements, risen after the claim - now completely discredited - of a link between the MMR vaccine and autism [5]. The occurrence of important episodic outbreaks in low-middle income settings [6] as well as in US and several European countries [7-10] strongly suggests that measles still represents a persisting major public health issue for both developing and developed countries.

Recent works have highlighted the importance of demographic processes in shaping the circulation of childhood infections [11-13] and the contribution of fertility trends in determining the local interruption of measles transmission [3,14]. Measles epidemiology varies widely across countries, and so do vaccination programs currently in place. To what extent the observed heterogeneity in measles epidemiology is related either to the effectiveness of country specific immunization activities or to the heterogeneity of key demographic components still represents an open question.

The aim of this work is to investigate inter-country differences in measles epidemiology by disentangling the impact of local demographic conditions and past demographic changes on the success of vaccination. To do this, we developed an age-structured transmission model informed with longitudinal data on country specific immunization activities, including routine programs, catch-up and follow-up campaigns, and by explicitly taking into account changes in demographic conditions (i.e., mortality and fertility) as occurred during the last 65 years. The proposed comparative study includes nine countries that are representative of regions at different stages of the demographic transition and are characterized by remarkably different vaccination histories against measles [2,15]: Australia, Ethiopia, Kenya, Ireland, Italy, the Republic of Korea, Singapore, the UK and US. The model is calibrated by exploring the likelihood of observing the reported age- and country-specific measles serological profiles by using a Markov chain Monte Carlo approach [16].

The current work differentiates from previous studies by explicitly modeling epidemiological transitions occurred over a rather long term, taking into account demographic processes and immunization strategies characterizing different socio-economic settings. Routine epidemiological surveillance mainly reports on clinically apparent cases of infection, while the population susceptibility and immunity represent hidden variables of the dynamics of infection. The adopted multi-country perspective gives significant insights on the current age-specific immunity profiles across different countries, and on the suitability of current vaccination strategies on the basis of local demographic and epidemiological patterns.

## **Materials and methods**

**Model structure.** Simulations of the demographic dynamics characterizing each

country were obtained by initializing the model with a population reflecting the age structure and population size observed in 1950 and by running the model for 65 consecutive years. Changes in local demographic conditions were simulated at the country level as informed with longitudinal data on variations of fertility, mortality and migration rates as reported by United Nations World Population Prospect ([\url{http://esa.un.org/unpd/wpp/}](http://esa.un.org/unpd/wpp/)), accessed Jan 2016). Demographic trends predicted across countries were validated against the age distributions of the population observed at different years and the reported variations in the overall number of individuals.

Measles transmission dynamics was simulated through a compartmental deterministic model structured in 8- 15year age classes. We assumed that maternal antibodies protect newborn individuals against measles infection for 6 months on average [6,17], after which they become susceptible and can get infected upon contacts with infectious individuals under the assumption of homogeneous mixing. Measles generation time was set to 14 days, on average [11]. Once recovered from natural infection, individuals gain permanent immunity against measles re-infection. Country specific routine first and second dose programs as well as nationwide Supplementary Immunization Activities (SIAs) were simulated by mimicking schedule and coverage data as reported by international organizations ([\url{http://www.who.int/immunization/}](http://www.who.int/immunization/)), accessed Jan 2016), complemented with national administrative records and recently published studies [10,18-20]. Immunization activities performed at a country level are summarized in Table 1. We assumed that only a fraction of vaccinated individuals develop immunity against measles infection and that for these individuals the vaccine-derived protection is life-long. Vaccine efficacy is assumed to be 85% when the vaccine is administered to individuals younger than 14 months, and 95% otherwise [21]. Only individuals who have been previously vaccinated with a first dose are considered eligible for a second dose, while all individuals can be vaccinated during a SIA. A detailed description of modeled epidemiological transitions for each individual's age can be found in the S1 Text.

**Model calibration and validation.** The transmission model was calibrated separately for each country, using available age specific serological profiles [18,19,22-27]. Free model parameters are represented by a country-specific measles transmission rate and a parameter used to adjust for the uncertainty on coverage levels associated with different SIAs when present [28,29]. A formal model evaluation, based on the deviance information criterion (DIC), shows that the inclusion of this latter parameter improves the model capability of reproducing the observed serological profiles (see S1 Text for further details). The demographic and transmission model was initialized according to the age structure of the population in 1950. The number of individuals in each of the epidemiological classes considered reflected the fraction of susceptible, infected and immune individuals associated with a certain transmission rate and the corresponding equilibrium solution obtained in the absence of vaccination. The latter was obtained by running the transmission model with constant fertility and mortality rates fixed to those observed in 1950, and by initializing the system with 10 infected individuals in a fully susceptible population.

Simulations of measles dynamics from 1950 to 2015 were obtained by running the model for 65 consecutive years, accounting for the time varying crude birth, net migration and age-specific mortality rates, and mimicking vaccination programs implemented during the considered period.

The posterior distribution of the free model parameters were estimated by means of a Markov chain Monte Carlo (MCMC) approach with random walk Metropolis–Hastings sampling [11,16] applied to the binomial likelihood of the observed country-specific measles serological profiles [18,19,22-27].

Convergence of MCMC was assessed by considering several different starting points and by visual inspection of 10,000 iterations, after a burn-in period of 2,000 iterations. More details on model calibration are provided in S1 Text.

## Results and Discussion

**Demographic processes underlying measles transmission.** Observed historical trends confirm that the considered countries reflect different stages of the "demographic transition" [15], i.e. changes in the population age structure due to the decline of fertility and death rates characterizing regions developing from a pre-industrial to an industrialized economic system. In particular, countries such as Italy, Korea and Singapore experienced a marked progressive aging of the population during the last 65 years. In these countries the percentage of individuals over 50 years of age increased from 8-22% in 1950 to 31-41% in 2015. On the opposite, countries like Kenya and Ethiopia exhibit a persisting young population (less than 14% above 50 years of age), although a decline of the percentage of pre-school children during the last 20 years is also detectable.

**Determinants of measles epidemiology.** The model was capable of satisfactorily reproducing the observed serological patterns for all countries. In particular, the derived root mean square error (RMSE) between model estimates and data was consistently below 10% (see Fig.1). A formal quantification of the goodness of fit can be found in the S1 Text.

The estimated posterior distributions of the transmission rate show significant differences across countries, with mean values ranging from 0.31days<sup>51</sup> in Kenya to 2.01days<sup>51</sup> in UK, possibly reflecting heterogeneities of social mixing patterns in the different regions. This hypothesis is partially supported by a significant positive Pearson correlation (p-values  $< 0.05$ ) between the average estimates of country-specific transmission rates and critical socio-demographic indicators such as the percentage of children attending primary and pre-primary school, the percentage of urbanized area, and GDPs (see S1 Text).

Interestingly, and in line with results reported in [28] and [29], we found that in countries where massive campaigns were performed, such as in Ethiopia, Kenya and Australia, coverage levels associated with SIAs were 20-35% lower than those reported, indicating that the impact of catch-up and follow-up campaigns is often overestimated. However, a high variability characterize obtained estimates of the coverage adjusting factor and the transmission rate, as summarized by the coefficient of variation characterizing their posterior distributions, ranging respectively from 0.04 to 1.3 and from 0.02 to 0.05. In particular, the extremely low coverage estimated for SIAs conducted in Ireland

may reflect difficulties in immunizing individuals who escaped both first and second dose routine vaccination.

Estimated temporal trends in measles circulation were found to be significantly correlated with WHO records of measles cases between 1974 and 2014 across the nine considered countries (see S1 Text for details). Our analysis shows that the progressive intensification of immunization efforts performed by different public health systems has remarkably reduced measles incidences with respect to pre-vaccination levels (see Fig.2): by 87% in Italy, 89% in US, 90% in UK and by more than 99% in the remaining countries. However, model results also suggest that the decline of fertility experienced over the past decades by more developed countries might have contributed to almost half of the reduction in incidence rates observed after the introduction of vaccination. This result was obtained by simulating an illustrative scenario where, in the absence of vaccination, the epidemiological transitions in the different countries were only determined by changes in fertility, mortality and migration rates. These simulations highlighted the impact of demographic processes alone on measles transmission dynamics. In particular, we found that, as already suggested from previous work [11-13], an increase of fertility rates is expected to produce a rise in the fraction of susceptible individuals in the host population, increasing measles circulation and decreasing the median age at infection. According to our simulations, this mechanism is valid for all countries considered, as proved by the high correlation we found between the crude birth rate and the predicted measles incidence over time (see Fig.2). The changes in measles epidemiology, however, result more pronounced in regions characterized by a faster demographic transition, such as Singapore and Korea, and less evident in those populations with a more stable age-structure, as is the case for Kenya (see Fig.3). Our analysis also highlight that countries and epochs associated with relatively lower fertility rates require less intense immunization efforts to achieve measles elimination. The relationship between measles transmission and fertility is investigated in detail in the S1 Text, where the predicted contribution of demographic trends in shaping measles circulation is validated empirically using long term Italian incidence data.

**Estimates on current immunity profiles.** By mimicking country-specific immunization programs performed during the last 30 years, we disentangled the relative contribution of different activities in reducing measles susceptibility for the nine considered countries. Fig.4 shows the epidemiological status estimated for 2015, highlighting for each age strata the percentage of individuals who are still susceptible to infection, who have experience the natural infection, who are protected by maternal antibodies, and who have been immunized either through routine programs (first and second dose) or SIAs.

According to our results, routine universal administration of first dose of measles vaccine has been responsible for more than 90% of the overall number of successfully immunized individuals in most countries. However, in Ethiopia and Kenya, catch-up and follow-up campaigns remarkably contributed to mitigate routine sub-optimal uptake, generating respectively about 45% and 25% of the immunized fraction of the population.

High levels of protection in Korea and Australia have been achieved by combining catch up campaigns with the introduction of a second booster dose. Although the contribution of a second booster dose to the total amount of immunized individuals is less than 7% for all countries considered, changes in the age at 2nd dose administration in Singapore (from 11 to 6 years of age in 2008 and from 6 years to 18 months in 2012), aimed at reducing measles infection in early childhood, have generated two persisting immunization gaps respectively between 4-7 and 11-17 years of age, corresponding to cohorts of individuals unprotected by both the current and the preceding schedules.

Model estimates suggest that, in all countries, naturally acquired immunity was progressively replaced by vaccine-induced immunity as a consequence of immunization efforts, so that measles natural infection has only partially filled immunity gaps caused by sub-optimal vaccination coverage. Remarkable differences among countries are predicted on the percentage of the population who acquired immunity from past natural infection, ranging from 36.4% in Kenya to 72.7% in Italy, and the estimated residual susceptibility in 2015 ranges from less than 3% of the overall population in Ireland to around 12.6% in Ethiopia (see S1 Text).

### **Towards measles elimination: priority targets for future immunization**

According to our estimates, more than 70% of susceptible individuals in Italy, US, Australia, Singapore and Korea are older than 5 years of age, and about 60% are older than 10 years. Although immunization activities targeting individuals older than 25 years would be certainly beneficial, for these countries it is essential to reduce the proportion of susceptible individuals among the adolescents and young adults through targeted catch-up campaigns.

Low routine vaccine uptake still persists in Ethiopia, where more than 60% of susceptible individuals are estimated to be less than 10 years of age, and in Kenya, where children under-five years represent about 40% of individuals exposed to the risk of infection. In these countries a remarkable fraction of young individuals has been vaccinated through SIAs. However, benefits coming from past campaigns are expected to eventually wane over time and even a local interruption of frequent follow-up programs may represent a major risk for these countries, where a significant increase of routine coverage levels is required to mitigate the progressive inflow of entire cohorts of individuals not adequately immunized.

Data coming from measles outbreaks often provide information only on local epidemiological conditions and may represent fragmentary evidence on the circulation of the infection in the population. This is the case of Korea, where erratic measles transmission has been reported between 2002 and 2011, as suggested by the small number of cases recorded during this period and huge fluctuations in the age-distribution of observed cases (see S1 Text).

Nonetheless, a comparison of the age distribution of reported measles cases across different countries between 2000 and 2014 [6-10,30] with the estimated age distribution of residual measles incidence shows that the RMSE between central model estimates and data is lower than 15% for 6 out of 7 considered countries and lower than 8% for 5 of these (see Fig.5). The overall compliance of

model predictions with these data, partially support the reliability of the provided indications on possible priority targets for future immunization efforts.

Current measles circulation among different ages is partially mirrored by the estimated median age at infection. Model results show the latter to be currently between 5 and 10 years of age in UK, Ireland, and Ethiopia; between 10 and 15 in US, Australia, Singapore and Kenya, and above 20 in Italy and Korea (see S1 Text). Temporal variations in measles transmissibility are mirrored by the dynamics of the effective reproduction number, defined as the expected number of secondary cases generated by one infected individual in a population partially immunized, either by vaccination or by natural infection [11]. Country-specific estimates of this quantity suggest that measles incidence may increase in Italy, Australia and Singapore and that the rapid increase of susceptibles currently ongoing in Ethiopia puts this country at higher risk of future outbreaks (see S1 Text).

Interestingly, our analysis suggest that, after the introduction of vaccination, the contribution of children less than 10 years to the effective reproductive number has progressively decreased as a consequence of the increase of individuals protected by vaccination. In particular, the decrease of measles circulation led by vaccination has gradually reduced infection rates among unvaccinated individuals, increasing the fraction of susceptibles at older ages and generating, in some countries, considerable immunity gaps among individuals between 30-40 years of age (see Fig.4). This phenomenon is expected to be more significant in countries where the fraction of adults in the population is higher. Indeed, despite remarkable levels of susceptibility among individuals between 25 and 40 years of age can be found in Kenya (see Fig.4), the overall contribution of young adults in the effective reproductive number appears marginal in this country. Further details on the expected temporal trends in the age-specific effective reproductive number across different countries can be found in SI Appendix.

## **Conclusion**

Any advance towards measles elimination will rely on the ability of public policies in decreasing the residual susceptibility inherited from the past, and in mitigating the natural replenishment of susceptibles due to new births. The multi-country perspective adopted in this study, and the explicit inclusion of time varying demographic components allow us to disentangle the contribution of different immunization activities and local demographic conditions in the progress towards measles elimination. We found that, beyond the effect of public health interventions, demographic changes dramatically contributed to the observed reduction of measles incidence rates after the introduction of vaccination.

In the long term, the attainment of high immunity levels in the population requires the achievement and maintenance of high routine vaccine uptake in children. However, our results also suggest that while in younger populations the residual susceptibility is mainly concentrated in early childhood, a considerable fraction of susceptibles individuals is found across all ages in countries characterized by lower fertility levels. From a policy making perspective, this



implies that routine childhood vaccination should be considered the key strategy to reduce measles circulation in less developed countries, where coverage levels associated with first-dose programs are often sub-optimal and where benefits of past catch-up campaigns are expected to rapidly wane over time. In fact, more marked variations in the immunized fraction of the overall population, as a consequence of changes in routine coverage, are likely to occur in countries associated with a younger age structure. This means that countries characterized by higher fertility rates can more rapidly achieve but also deviate from a target level of immunization. On the contrary, immunization campaigns targeting adolescents (and possibly young adults) are essential to achieve measles elimination in more developed areas, where the effect of past immunization activities, either beneficial or detrimental, are expected to weight more as a consequence of a slower generational replacement.

The paucity of epidemiological data associated with different time points, and the assumptions of homogeneous mixing and a constant transmission rate over time are three critical limitations of the proposed investigation.

Unfortunately, data on realistic social mixing patterns by age are not available for all considered countries and different epochs. However, a recent modeling work has shown that the inclusion of static estimates on mixing patterns by age in a similar model does not affect yearly incidence trends over time [11].

In addition, the effects of the explicit inclusion of seasonal variations in measles transmission due to school terms was considered in a sensitivity analysis (see S1 Text) and shown not to affect neither the predicted temporal trends in yearly incidence rates nor the longitudinal changes in the population immunity profiles over a rather long term.

The analysis of different incidence records - though representing only a fraction of the infected cases - provide complementary epidemiological evidences supporting the epidemiological patterns identified by our analysis.

Available serological data for Ethiopia and Kenya may reflect only local epidemiological conditions so that obtained results for these two countries should be carefully considered as representative at a national level. Possible within country heterogeneities due to geographical differences in vaccine uptake were investigated simulating measles epidemiological transition in a low- and a high-coverage area of Ethiopia using data available at a regional level (see S1 Text for further details). The percentage of susceptible individuals under-five years of age was found to be highly variable within the country, ranging from 29.7% to 53.7%, possibly resulting into local episodic outbreaks, as those recently reported in Ethiopia [6].

Although the proposed model is not suited to make predictions on the likelihood of future occurrence of outbreaks, the obtained results provide critical indications on the main determinants of measles epidemiology across settings characterized by different demographic and socio-economic conditions.

Our results strongly indicate that a change of current measles control strategies is required, and that specific demographic conditions should be considered as a natural ingredient for future policy decision-making processes.

## Acknowledgments

The research leading to these results has received funding from the European Research Council under the European Union's Seventh Framework Programme (FP7/2007- 2013)/ERC Grant agreement n.2839-5 (DECIDE) to PP and AM.

## Authors' contributions

FT, PP, AM conceived and designed the experiments. FT, PP performed the experiments and drafted the first version of the manuscript. All authors contributed to the interpretation of the results, edited and approved the final manuscript. FT and PP contributed equally to this work. The funders had no role in study design, data collection and analysis, decision to publish, or preparation of the manuscript.

## Conflict of interest

The authors declare no conflict of interest.

## References

- [1] WHO. Global Measles and Rubella strategic plan. WHO Bulletin. 2012
- [2] Simons E, Ferrari M, Fricks J, Wannemuehler K, Anand A, Burton A, et al. Assessment of the 2010 global measles mortality reduction goal: results from a model of surveillance data. *The Lancet*. 2012;379(9832):2173-2178
- [3] Ferrari MJ, Grais RF, Bharti N, Conlan AJ, Bjornstad ON, Wolfson LJ, et al. The dynamics of measles in sub-Saharan Africa. *Nature*. 2008;451(7179):679-684
- [4] Katz SL, De Quadros CA, Izurieta H, Venczel L, Carrasco P. Measles eradication in the Americas: progress to date. *J Infect Dis*. 2004;189:S227-S233
- [5] Taylor B, Miller E, Farrington C, Petropoulos MC, Favot-Mayaud I, Li J, et al. Autism and measles, mumps, and rubella vaccine: no epidemiological evidence for a causal association. *The Lancet*. 1999;353(9169):2026-2029
- [6] Goodson JL, Masresha BG, Wannemuehler K, Uzicanin A, Cochi S. Changing epidemiology of measles in Africa. *J Infect Dis*. 2011;204(suppl 1):S20--S214
- [7] Hinman AR, Yip FY, Papania MJ, Redd SB. Measles outbreak epidemiology in the United States, 1993-2001. *J Infect Dis*. 2004;189(Supplement 1):S-4-S60
- [8] Filia A, Tavilla A, Bella A, Magurano F, Ansaldi F, Chironna M, et al. Measles in Italy, July 2009 to September 2010. *Euro Surveill*. 2011;16(29):1992-
- [9] Gee S, Cotter S, O'Flanagan D. Spotlight on measles 2010: measles outbreak in Ireland 2009-2010. *Euro Surveill*. 2010
- [10] Vivancos R, Keenan A, Farmer S, Atkinson J, Coffey E, Dardamassis E, et al. An ongoing large outbreak of measles in Merseyside, England, January to June 2012. *Euro Surveill*. 2012;17(29):20226

- [11] Merler S, Ajelli M. Deciphering the relative weights of demographic transition and vaccination in the decrease of measles incidence in Italy. *Proc R Soc Lond B*. 2014;281(1777):20132676
- [12] Marziano V, Poletti P, Guzzetta G, Ajelli M, Manfredi P, Merler S. The impact of demographic changes on the epidemiology of herpes zoster: Spain as a case study. *Proc R Soc Lond B*. 201-;282(1804):20142-09
- [13] Earn DJD, Rohani P, Bolker BM, Grenfell BT. A simple model for complex dynamical transitions in epidemics. *Science*. 2000;287(5453):6675670
- [14] Ferrari MJ, Grenfell BT, Strebel PM. Think globally, act locally: the role of local demographics and vaccination coverage in the dynamic response of measles infection to control. *Phil Trans R Soc B*. 2013;368(1623)
- [15] Casterline JB. The pace of fertility transition: national patterns in the second half of the twentieth century. *Pop and Dev Review*. 2001;27:17552
- [16] Cauchemez S, Carrat F, Viboud C, Valleron AJ, Boelle PY. A Bayesian MCMC approach to study transmission of influenza: application to household longitudinal data. *Stat Med*. 2004;23(22):3469-3487
- [17] Salmaso S, Gabutti G, Rota MC, Giordano C, Penna C, Mandolini D, et al. Pattern of susceptibility to measles in Italy. Serological Study Group. *Bull World Health Organ*. 2000;78(8):9-05955
- [18] Gilbert GL, Escott RG, Gidding HF, Turnbull FM, Heath TC, McIntyre PB, et al. Impact of the Australian Measles Control Campaign on immunity to measles and rubella. *Epidemiol Infect*. 2001;127(2):2975303
- [19] Ho HJ, Low C, Ang TW, Cutter JL, Tay J, Chan KP, et al. Progress towards measles elimination in Singapore. *Vaccine*. 2014;32(51):692756933
- [20] Hinman AR, Kolasa MS, Klemperer S, Johnson S, Papania MJ. Progress toward implementation of a second-dose measles immunization requirement for all schoolchildren in the United States. *Journal of Infectious Diseases*. 2004;189(Supplement 1):S985S103
- [21] De Serres G, Boulianne N, Meyer F, Ward B. Measles vaccine efficacy during an outbreak in a highly vaccinated population: incremental increase in protection with age at vaccination up to 18 months. *Epidemiology and Infection*. 1995;115(02):3155323
- [22] Kim SS, Han HW, Go U, Chung HW. Sero-epidemiology of measles and mumps in Korea: impact of the catch-up campaign on measles immunity. *Vaccine*. 2004;23(3):2905297
- [23] Hutchins SS, Bellini WJ, Coronado V, Jiles R, Wooten K, Deladisma A. Population immunity to measles in the United States, 1999. *J Infect Dis*. 2004;189:S91597
- [24] Nokes DJ, Enquselassie F, Nigatu W, Vyse AJ, Cohen BJ, Brown DW, et al. Has oral fluid the potential to replace serum for the evaluation of population immunity levels? A study of measles, rubella and hepatitis B in rural Ethiopia. *Bull World Health Organ*. 2001;79(7):5885595
- [25] Ohuma EO, Okiro EA, Bett A, Abwao J, Were S, Samuel D, et al. Evaluation of a measles vaccine campaign by oral-fluid surveys in a rural Kenyan district: interpretation of antibody prevalence data using mixture models. *Epidemiol Infect*. 2009;137(2):2275233
- [26] Andrews N, Tischer A, Siedler A, Pebody RG, Barbara C, Cotter S, et al. Towards elimination: measles susceptibility in Australia and 17 European countries. *Bull World Health Organ*. 2008;86(3):1975204

[27] Santoro R, Ruggeri FM, Battaglia M, Rapicetta M, Grandolfo ME, Annesi I, et al. Measles epidemiology in Italy. *Int J Epidemiol.* 1984;13(2):2015209

[28] Lessler J, Metcalf CJE, Grais RF, Luquero FJ, Cummings DA, Grenfell BT. Measuring the performance of vaccination programs using cross-sectional surveys: a likelihood framework and retrospective analysis. *PLoS Med.* 2011;8(10):e1001110

[29] Lessler J, Metcalf CJE, Cutts FT, Grenfell BT. Impact on epidemic measles of vaccination campaigns triggered by disease outbreaks or serosurveys: a modeling study. *PLoS Med.* 2016;13(10):e1002144

[30] Choe YJ, Bae GR. Current status of measles in the Republic of Korea: an overview of case-based and seroepidemiological surveillance scheme. *Korean journal of pediatrics.* 2012;55(12):4555461

## Figures and tables:

**Table 1. Immunization activities performed at a country level.**

Country	1 <sup>st</sup> dose	2 <sup>nd</sup> dose	SIAs
Australia	12m	4y	1998
Ethiopia	9m	5	2005, 2006, 2008, 2010
Ireland	12m	4y	1995, 2009, 2013
Italy	18m	5y	2005
Kenya	9m	5	2003, 2006, 2009, 2012
Rep. Korea	12m	4y	2001
Singapore	12m	18m*	5
UK	12m	5y	2013
US	15m	5y	5

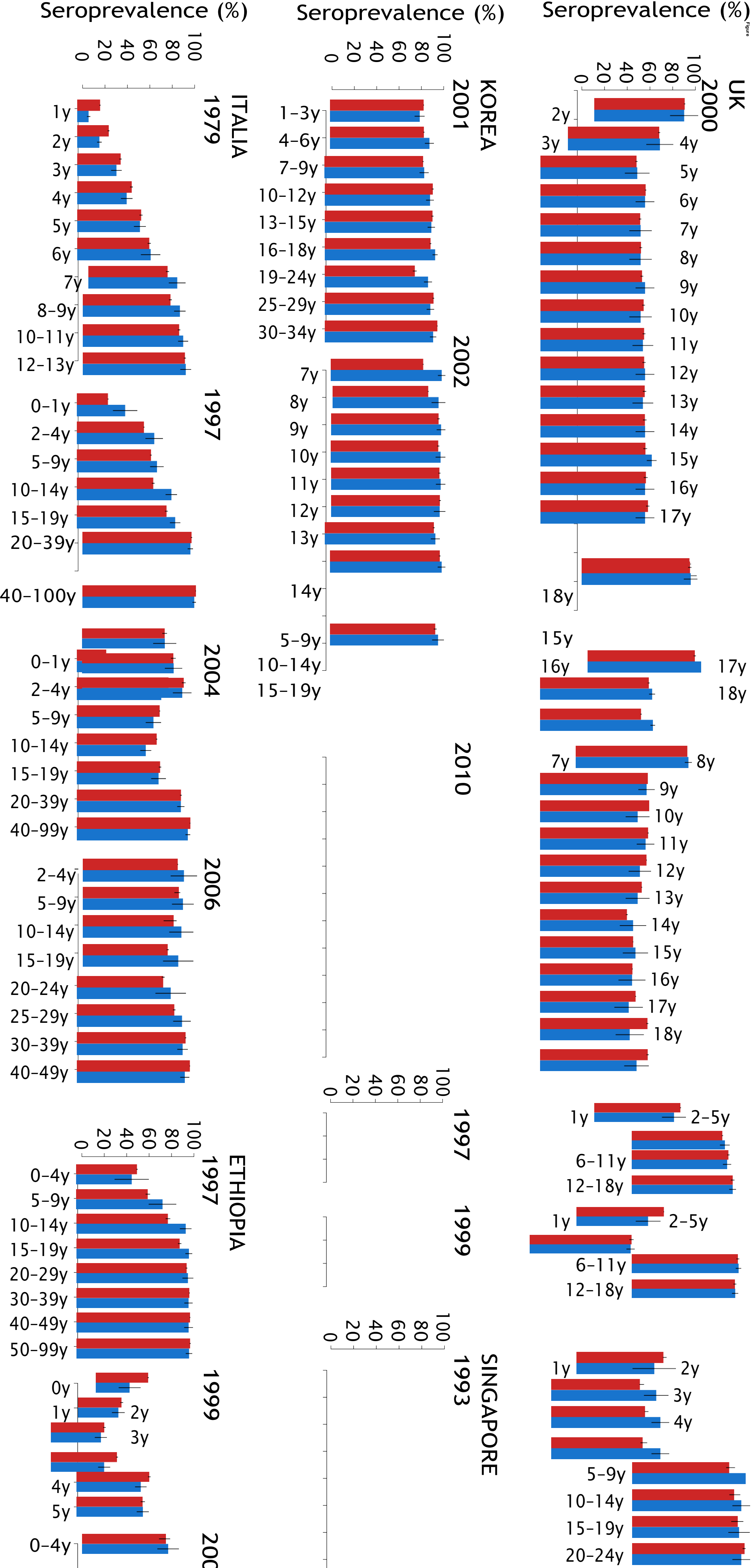
\* second dose was initially administered at 11 years of age, and progressively moved at 6 years of age in 2007 and at 18 months in 2011.

**Fig 1. Model calibration.** Predicted (red boxes) and observed (blue boxes) age specific serological profiles in different countries. Vertical lines represent 95% credible intervals associated with data records and model predictions.

**Fig 2. Temporal trends in measles circulation. a)** Model predictions on yearly measles incidence rates per 1,000 individuals over time, averaged over a moving window of 7 years (blue line) and the same quantity as predicted by the model in the absence of vaccination (green line), shown along with the reported crude birth rate (red line). Shaded areas represent 95% credible intervals associated with model predictions. **b)** The impact of demographic processes on measles epidemiology: barplots show the simulated average measles seroprevalence in the absence of vaccination among individuals at 5 (cyan), 10 (light blue) and 20 (dark blue) years of age for 1950, 1980, and 2015. Vertical bars show 95% of credible intervals.

**Fig 3. Estimated immunity profiles.** Model predictions on the epidemiological status at different ages and in different countries for 2015. For each age strata it is shown the percentage of individuals susceptible to infection (dark grey), protected against infection by immunity provided by maternal antibodies (light grey), and acquired through natural infection (cyan), routine first dose vaccination (yellow), second booster administration (orange) and SIAs (red).

**Fig 4. Model validation.** Distribution of measles cases as observed (blue) and as predicted by model simulation (green) among different age classes. Vertical bars show 95%CI.



25-34y  
35-44y

19y  
20-34y

5-9y  
10-14y

0 20 40 60 80 100

IRELAND  
1992 2003

3-6y  
7-10y  
11-14y

1y

2y

3y

4y

5y

6y

7y

8y

9y

10y

11y

12y

13y

14y

15y

16y

17-85y

AUSTRALIA

0 20 40 60 80 100

US  
2004

6-17y

18-27y

28-37y

38-55y

0 20 40 60 80 100

KENYA  
2001 2002

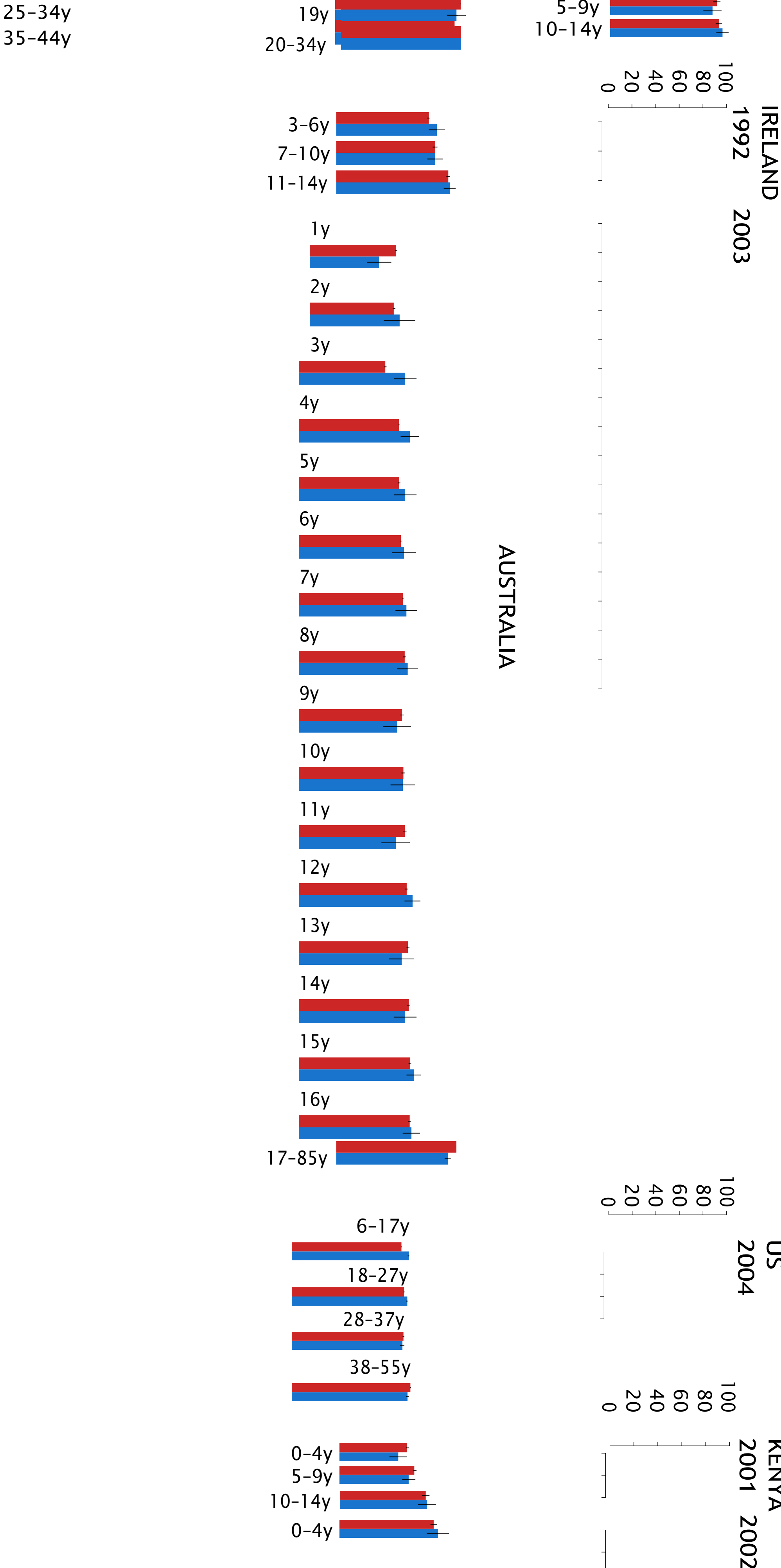
0-4y

5-9y

10-14y

0-4y

0 20 40 60 80 100



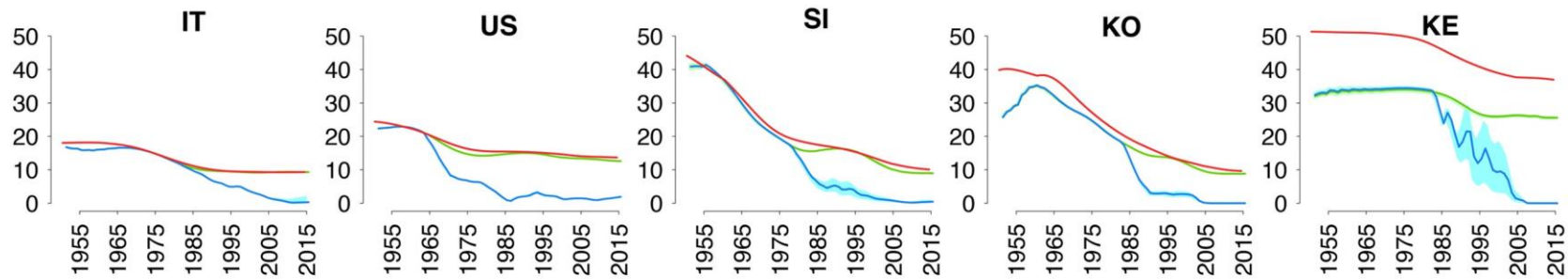
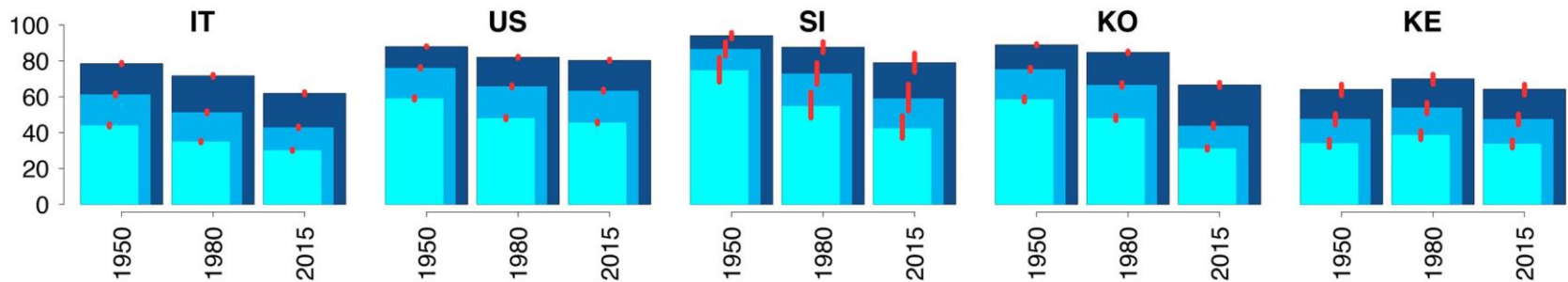
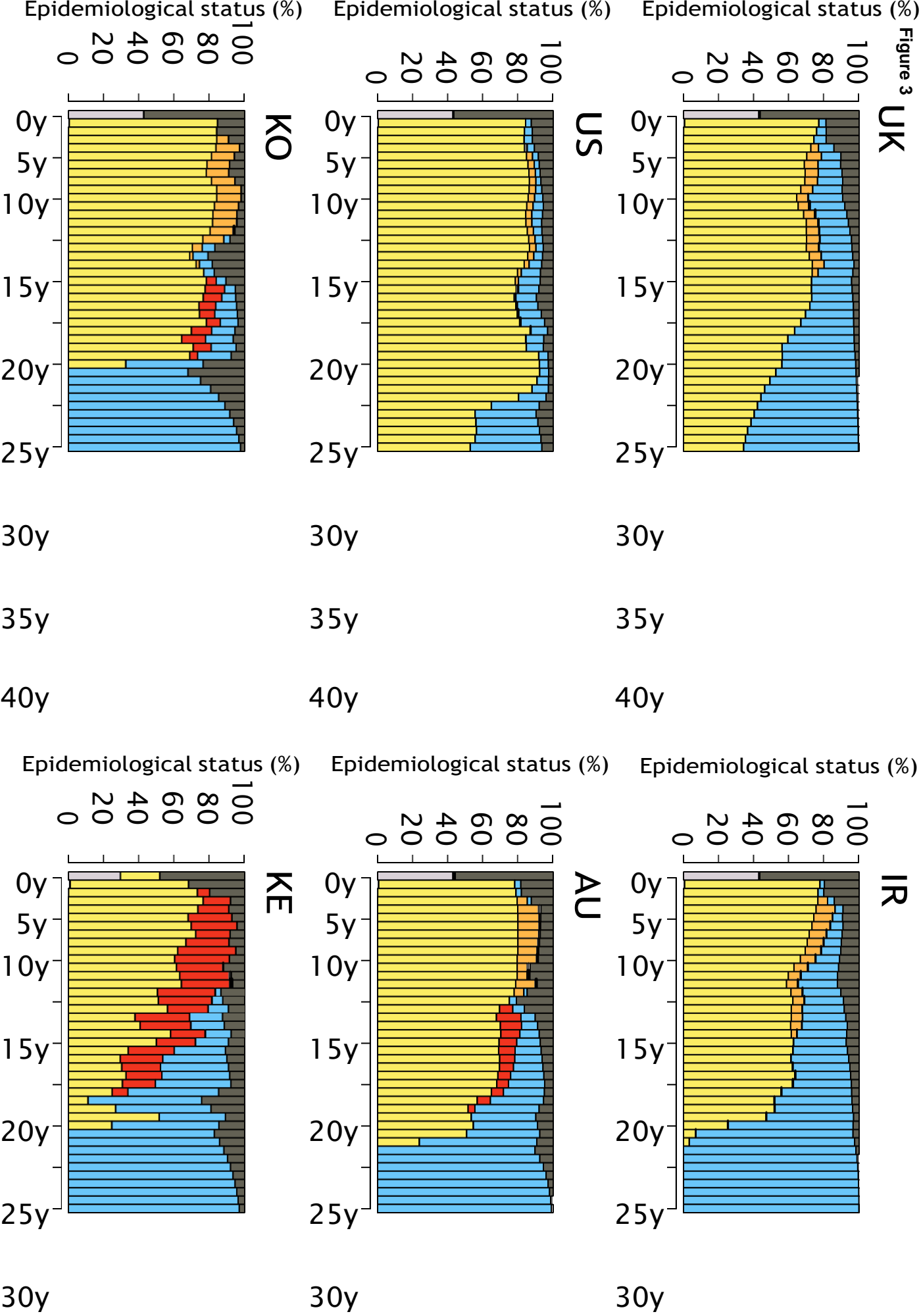
**Figure 2****a)****b)**

Figure 3





35y

35y

35y

40y

40y

40y

Epidemiological status (%)

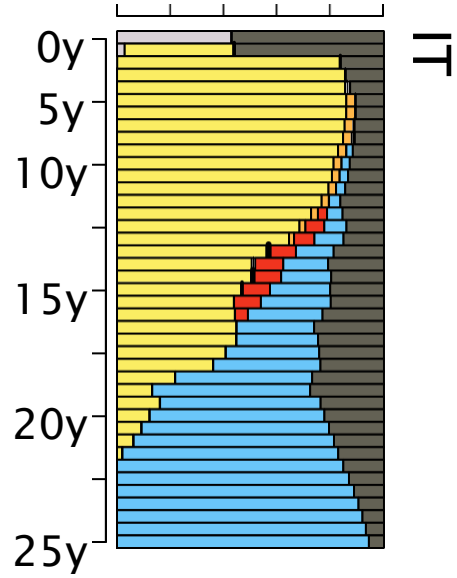
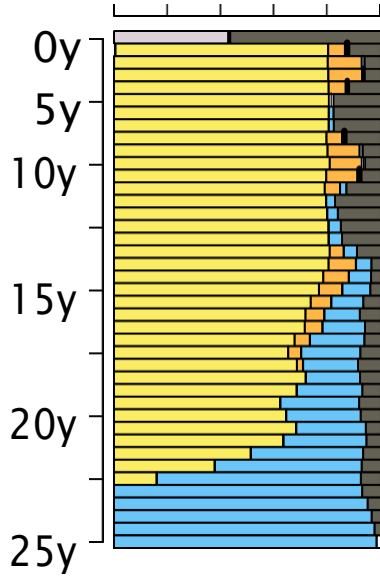
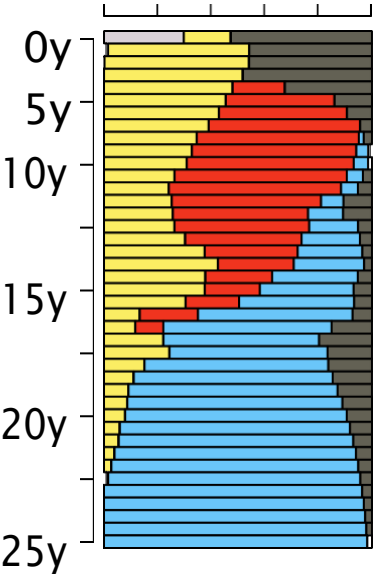
Epidemiological status (%)

Epidemiological status (%)

0 20 40 60 80 100

0 20 40 60 80 100

0 20 40 60 80 100



30y

30y

30y

35y

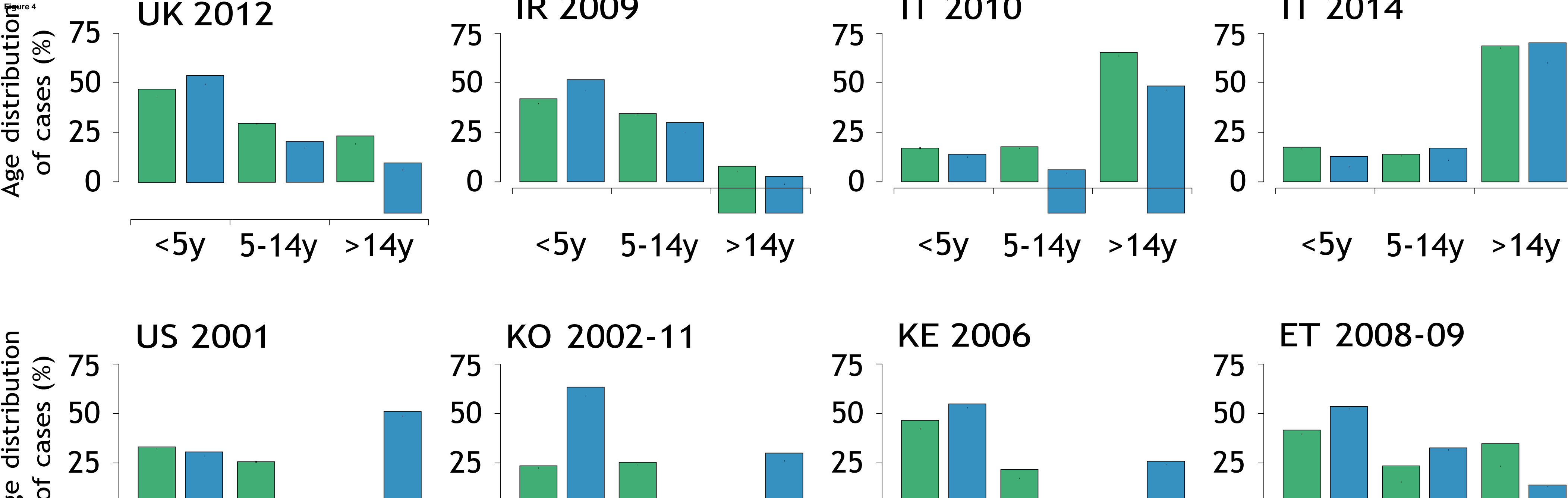
35y

35y

40y

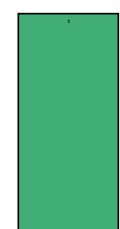
40y

40y



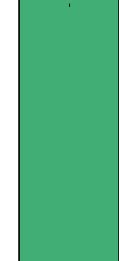
0

<5y 5-14y >14y



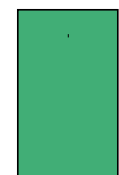
0

<5y 5-14y >14y



0

<5y 5-14y >14y



0

<5y 5-14y >14y



# Measles immunity gaps and the progress towards elimination: a model-based multi-country perspective.

Filippo Trentini<sup>1</sup>, Piero Poletti<sup>1,2</sup>, Stefano Merler<sup>2</sup> and Alessia Melegaro<sup>1,3</sup>

<sup>1</sup> DONDENA Centre for Research on Social Dynamics, Bocconi University, Milan, Italy,

<sup>2</sup> Center for Information Technology, Bruno Kessler Foundation, Trento, Italy.

<sup>3</sup> Department of Policy Analysis and Public Management, Bocconi University, Milan

## S1 Text

### Contents

1. Materials and methods
  - 1.1. The non-stationary age-structured transmission model
  - 1.2. Demographic data
  - 1.3. Epidemiological data
  - 1.4. Socio economic indicators
  - 1.5. Model calibration
  - 1.6. Model validation
  - 1.7. Sensitivity analysis
  
2. Additional results
  - 2.1. Measles transmission and socio-economic indicators
  - 2.2. Measles transmissibility potential
  - 2.3. Measles transmission and fertility trends
  - 2.4. Temporal changes in measles epidemiology
  - 2.5. Within country heterogeneity: the case of Ethiopia
  - 2.6. Current epidemiology of measles among different countries

# 1. Materials and methods

## 1.1 The non-stationary age-structured transmission model

Measles transmission is simulated through a deterministic non-stationary age-structured model stratified in 85-years age classes and based on the assumption of homogeneous mixing. The population is divided into different compartments: individuals protected by maternal antibodies ( $M$ ), susceptible individuals ( $S$ ), vaccinated individuals who were not successfully immunized due to vaccine failure ( $F$ ), infectious individuals ( $I$ ) and individuals who acquired immunity against measles either through vaccination or natural infection. Among the latter we kept trace of individuals who gained immunity after recovery from measles infection ( $R$ ) and individuals who were successfully immunized through first dose ( $V_1$ ), second booster ( $V_2$ ) and Supplementary Immunization Activities ( $V_{SIA}$ ).

Newborn individuals are protected against measles infection for 6 months on average by the passive transfer of maternal immunity after which they become susceptible. Each susceptible individual is exposed to the risk of infection through contacts with infectious individuals. Once infected, individuals enter the infectious compartment and contribute to the spread of infection. We assume a generation time of 14 days. In the model individuals are vaccinated according with data reported on immunization schedules and coverage levels, by mimicking country-specific vaccination activities performed from 1950 to 2015.

The model takes into account the vital dynamics of the host population, and is informed by country-specific crude birth rate, age-specific mortality rates and migration flows observed in the period considered.

Epidemiological transitions for each individual's age are described by the following system of ordinary differential equations:

$$\left\{ \begin{array}{l}
 \frac{dM(a, t)}{dt} = \lambda_{a,0} b(t) \sum_{j=10}^{85} n(j, t) - \mu M(a, t) - s(a) \left( \lambda_{a,a_1} c_1(t) + \sum_{j=a_{s1}}^{a_{s2}} \lambda_{a,j} c_s(t) \right) M(a, t) - d(a, t) M(a, t) \\
 \frac{dS(a, t)}{dt} = \mu M(a, t) - \beta S(a, t) \frac{\sum_{j=10}^{85} I(j, t)}{\sum_{j=10}^{85} n(j, t)} - s(a) \left( \lambda_{a,a_1} c_1(t) + \sum_{j=a_{s1}}^{a_{s2}} \lambda_{a,j} c_s(t) \right) S(a, t) - d(a, t) S(a, t) \\
 = (1 - s(a)) \lambda_{a,a_1} c_1(t) (S(a, t) + M(a, t)) - \beta F(a, t) \frac{\sum_{j=10}^{85} I(j, t)}{\sum_{j=10}^{85} n(j, t)} - s(a) \left( \lambda_{a,a_2} c_2(t) + \sum_{j=a_{s1}}^{a_{s2}} \lambda_{a,j} c_s(t) \right) F(a, t) - d(a, t) F(a, t) \\
 \frac{dI(a, t)}{dt} = \beta S(a, t) + F(a, t) \frac{\sum_{j=10}^{85} I(j, t)}{\sum_{j=10}^{85} n(j, t)} - \lambda(a, t) - d(a, t) I(a, t) \\
 \frac{dR(a, t)}{dt} = \lambda(a, t) - d(a, t) R(a, t) \\
 \frac{dV_1(a, t)}{dt} = s(a) \lambda_{a,a_1} c_1(t) S(a, t) + M(a, t) - d(a, t) V_1(a, t) \\
 \frac{dV_2(a, t)}{dt} = s(a) \lambda_{a,a_2} c_2(t) F(a, t) - d(a, t) V_2(a, t) \\
 \frac{dV_{SIA}(a, t)}{dt} = s(a) \sum_{j=a_{s1}} \lambda_{a,j} c_s(t) (S(a, t) + M(a, t) + F(a, t)) - d(a, t) V_{SIA}(a, t) \\
 n(a, t) = M(a, t) + S(a, t) + F(a, t) + I(a, t) + R(a, t)
 \end{array} \right.$$

where  $t$  and  $a$  represent time and individuals' chronological age respectively;  $1/\mu$  is the average duration of protection provided by maternal antibodies;  $\beta$  is the measles transmission rate;  $1/\gamma$  is the average duration of the infectivity period;  $b(t)$  and  $d(a,t)$  are the crude birth rate and age-specific mortality rate at time  $t$  respectively. Coverage levels at time  $t$  associated with first dose and second dose programs are denoted by

$c_1(t)$  and  $c_2(t)$  respectively;  $c_s(t)$  is the vaccination coverage characterizing supplementary immunization activities performed at time  $t$  and targeting ages between  $a_{s1}(t)$  and  $a_{s2}(t)$ ;  $\varepsilon(a)$  represents the vaccine efficacy, which depends on the age at vaccine administration. Finally,  $N(a,t)$  represents the total population of age  $a$  at time  $t$  and  $\delta_{a,j}$  is the Dirac delta function, equal to 1 for  $a=j$  and 0 otherwise.

## 1.2 Demographic data

The model was informed with country specific longitudinal data on crude birth rates (Fig. S1), age specific mortality rates (Fig. S2 and S3) as reported by United Nations World Population Prospect [1] and migration flows as estimated by combining the reported net migration rates (Fig. S4) [1] and age distribution of migrants [2].

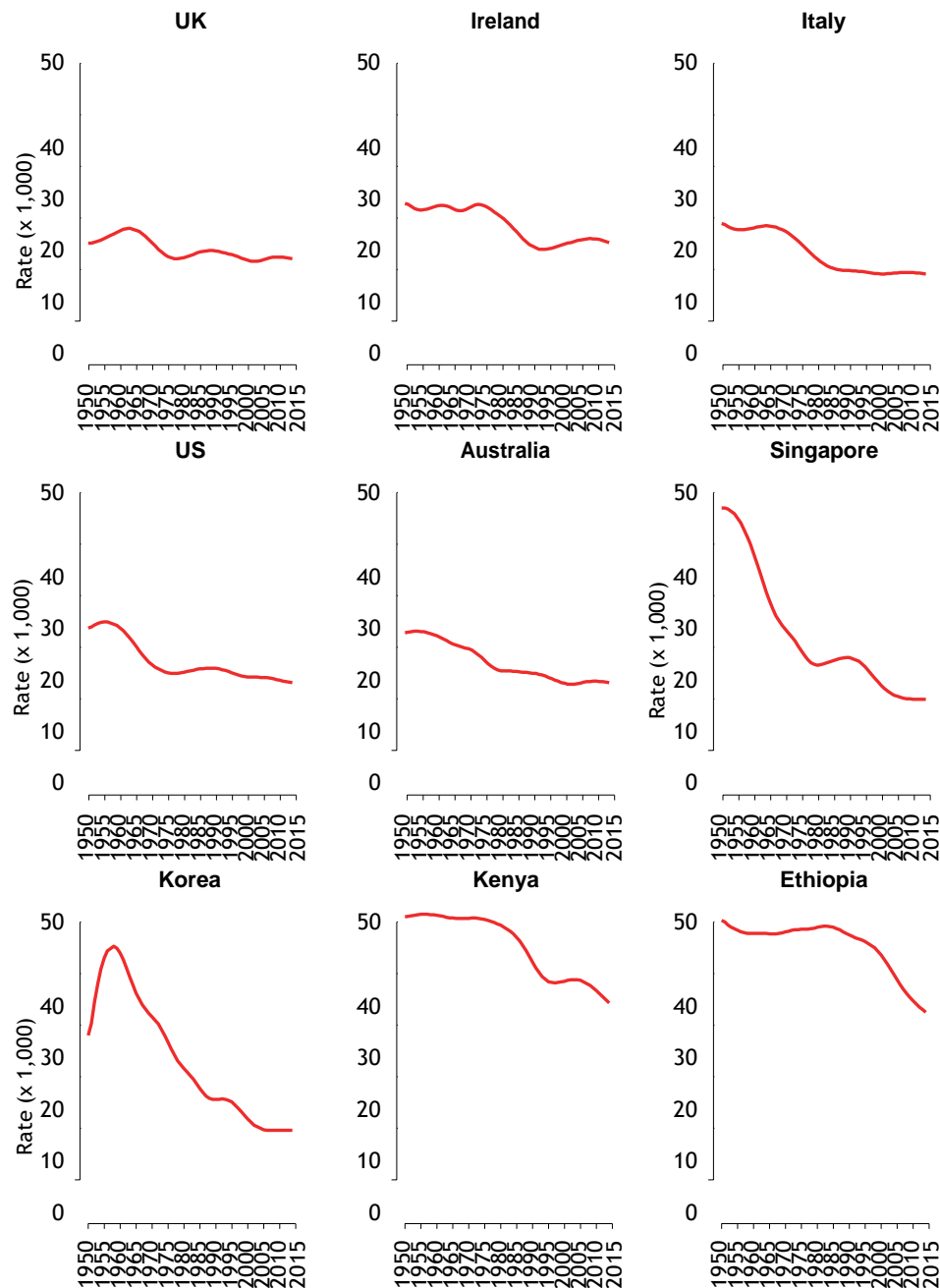


Fig. S1 Reported crude birth rate.

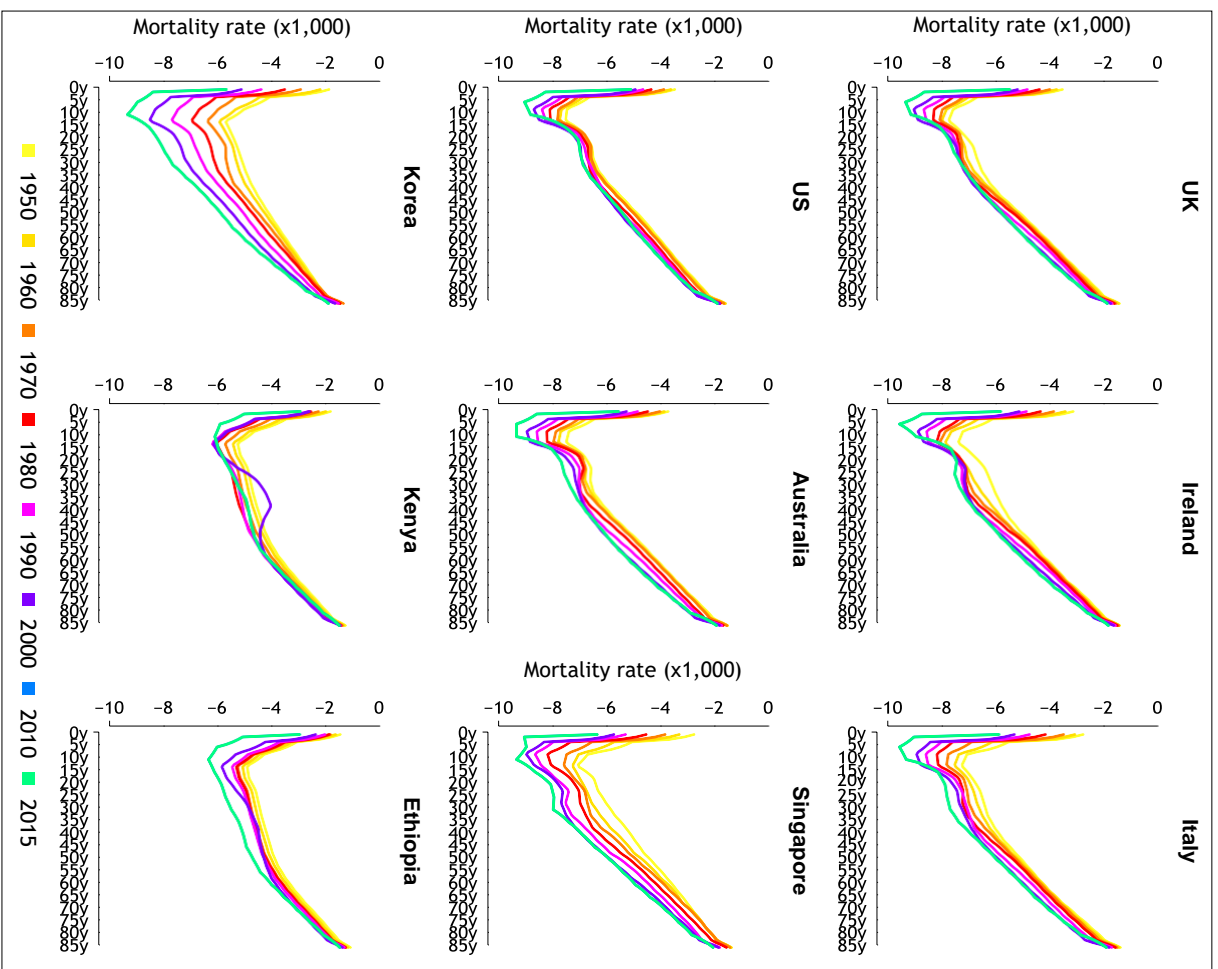


Fig. S2 Data on country specific mortality rates by age at different time points.

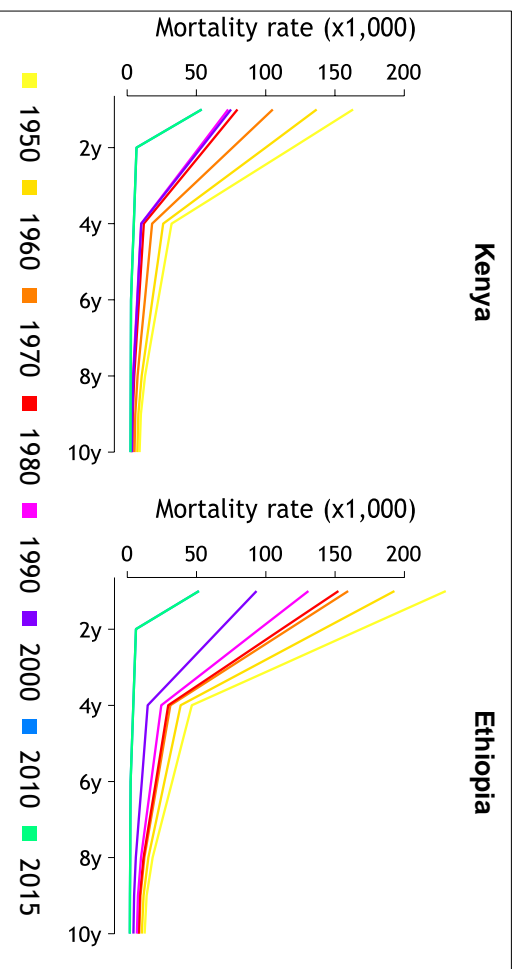
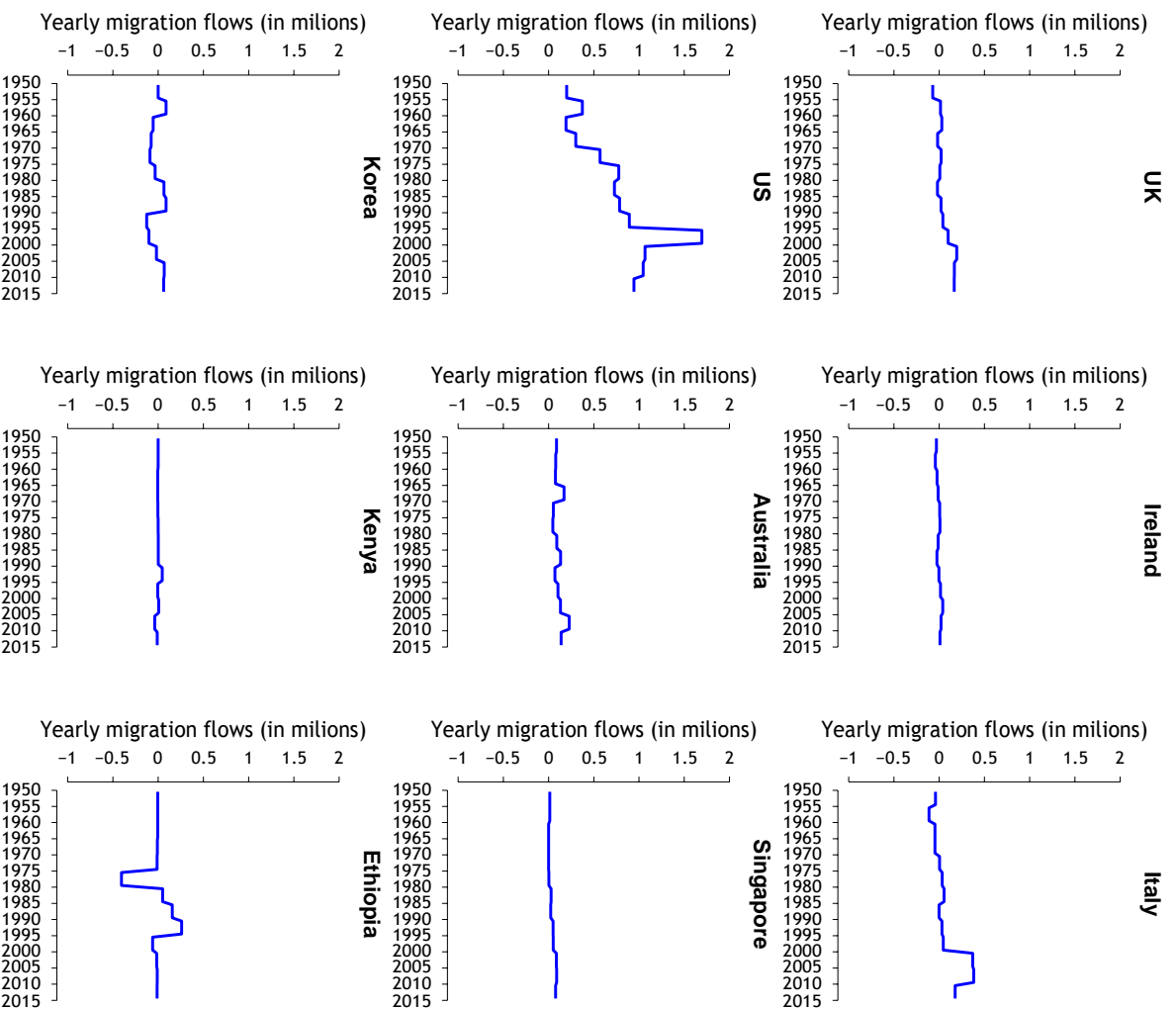


Fig. S3 Data on mortality rates among individuals younger than 10 years of age in Kenya and Ethiopia.





**Fig. S4 Data on yearly net migration flows**

In order to obtain annual mortality rates associated with each age considered in the model, data on mortality rates available for every 5 years from 1950 to 2015 and different age classes were interpolated along years and different ages. The number of migrants by age was approximated multiplying the net yearly migration flows (Fig. S4) by the age distribution of migrants, available for three different time points (Fig. S5).

The model is able to well reproduce main demographic processes occurred between 1950 and 2015 in all countries under study, in terms of the age structure and the total size of the host population. Model validation against available data is shown in Fig. S6 and S7.

In particular, according to demographic historical trends, countries such as Italy, Korea and Singapore experienced a marked progressive ageing of the population during the last 65 years. In these countries the percentage of individuals over 50 years

of age increased from 8-22% in 1950 to 31-41% in 2015. On the opposite, during the considered period, countries like Kenya and Ethiopia exhibit a persisting young population (less than 14% above 50 years of age), although a decline of the percentage of pre-school children during the last 20 years is also detectable.

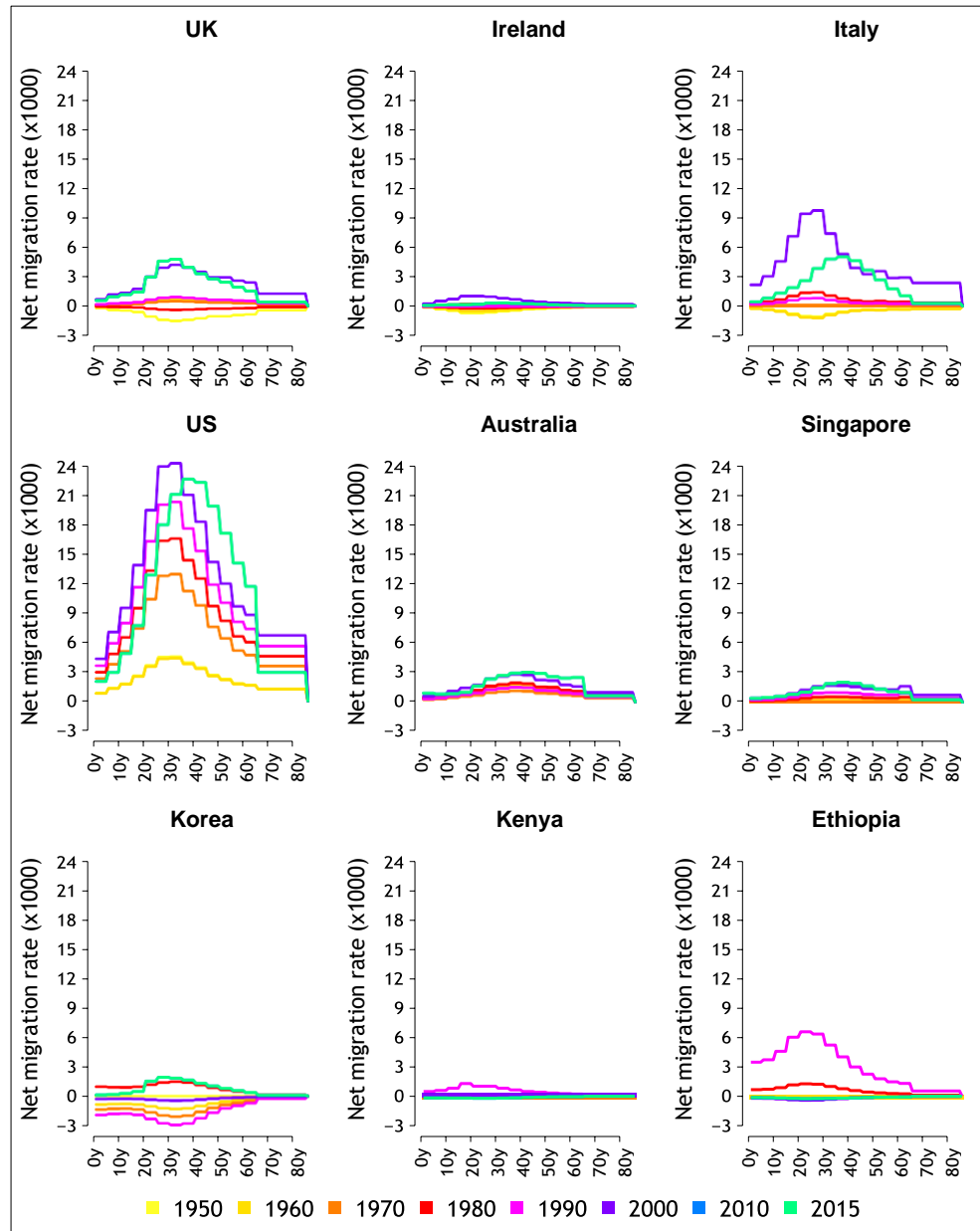
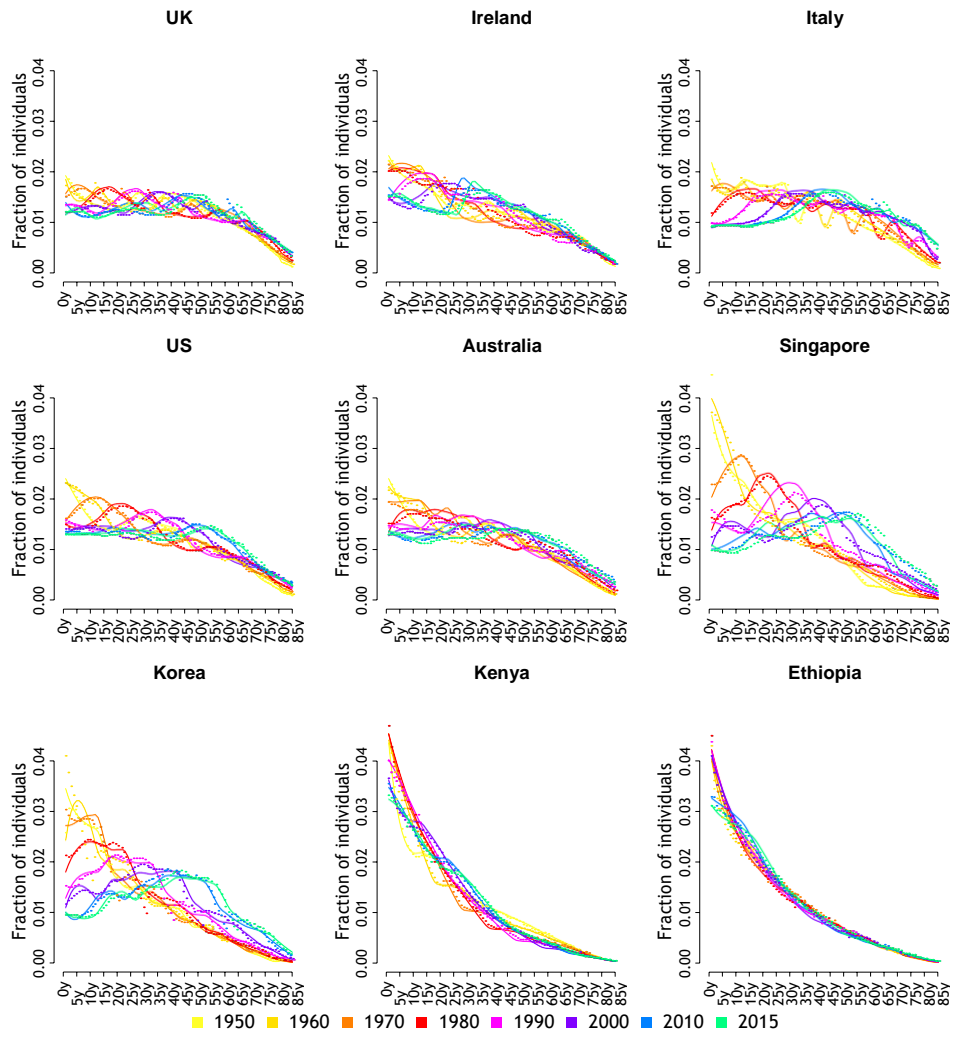
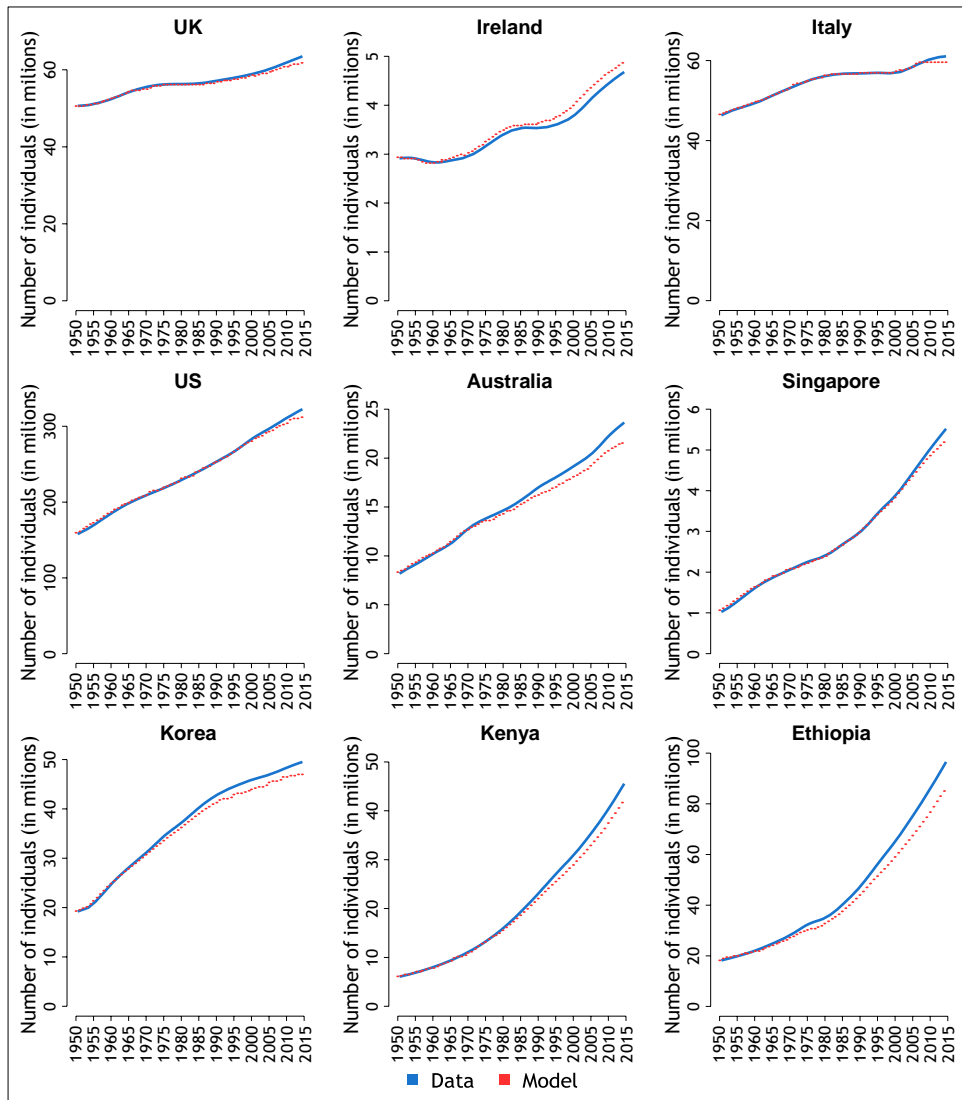


Fig. S5 Data on temporal trends in the number of migrants by age (1950-2015)



**Fig. S6 Evolution of the population age structure over time: model (lines) vs data (points).**

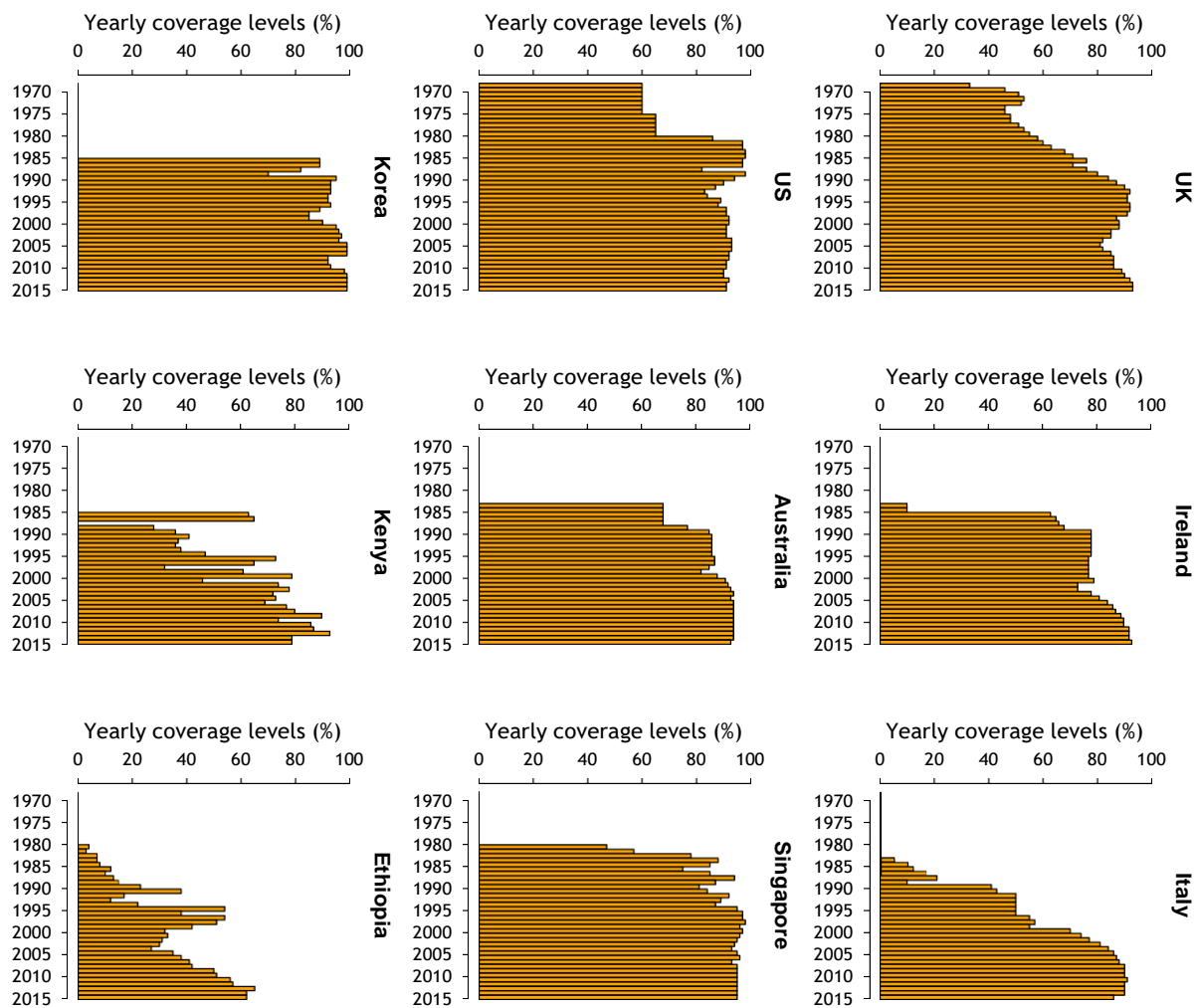


**Fig. S7 Evolution of the population size over time: model (red points) vs data (blue line)**

### 1.3 Epidemiological data

Country specific vaccination strategies were simulated, by accounting for first dose vaccination, second dose administration, and supplementary immunization activities performed over the years. Data on first and second dose were obtained from data and estimates reported by international organizations [3], and complemented for Italy with administrative records of the Italian Ministry of Health [4] and for US with data reported in [5]. Coverage levels for first dose are shown in Fig. S8.

Fig. S8 Routine coverage levels associated with the 1<sup>st</sup> dose program among different countries.



Vaccination schedule associated with routine programs are reported in Tab. S1 along with the year of introduction of first dose and second booster.

COUNTRY	1st DOSE introduction	AGE AT 1st DOSE	2nd DOSE introduction	AGE AT 2nd DOSE
Australia	1983	12 months	2004	4 years
Ethiopia	1980	9 months	--	--
Ireland	1983	12 months	1999	4 years
Italy	1983	18 months	1999	5 years
Kenya	1985	9 months	--	--
Rep. Korea	1985	12 months	2000	4 years
Singapore	1980	12 months	1999	18 months *
UK	1968	12 months	2000	5 years
US	1965	15 months	1991	5 years

(\*) the second dose was initially administered at 11 years of age, and progressively hastened in 2007 at 6 years of age and at 18 months in 2011

**Tab. S1 Routine vaccination programs (1<sup>st</sup> dose and second booster) in the considered countries.**

Supplementary immunization activities performed across different countries (and explicitly accounted for) are summarized in Tab. S2.

COUNTRY	YEAR OF SIA	TARGETED AGE GROUPS	REFERENCES
Australia	1998	1 to 12 years	[6]
Ethiopia	2000	1 to 5 years	[7]
Ethiopia	2005	1 to 14 years	[8]
Ethiopia	2006	1 to 5 years	[8]
Ethiopia	2008	1 to 5 years	[8]
Ethiopia	2010	1 to 5 years	[3]
Ireland	1995	5 to 12 years	[9]
Ireland	2009	15 to 18 years	[10]
Ireland	2013	5 to 18 years	[11, 12]
Italy	2005	6 to 13 years	[13]
Kenya	2003	1 to 14 years	[14]
Kenya	2006	1 to 5 years	[14]
Kenya	2009	1 to 5 years	[15]
Kenya	2012	1 to 5 years	[16]
Rep. Korea	2001	8 to 16 years	[17]
UK	2013	10 to 16 years	[18]

**Tab. S2 Supplementary immunization activities performed between 1980 and 2015 in the considered countries.**

A recent review on measles vaccination [19] shows that estimates of measles vaccine efficacy among children immunized at 15 months or older is between 94% and 100%, and between 43% and 85% when the vaccine was administered under 9 months of age. Critically low levels of vaccine efficacy found in some developing countries have been explained in terms of either too young an age at vaccination or a poor cold chain. However, age of vaccination is considered as the most important factor in measles vaccine effectiveness. Low effectiveness when the vaccine is administered at low ages has been explained by the presence of maternal antibodies against measles in infants interfering with the seroconversion to measles vaccine. Our assumptions on vaccine efficacy are based on results found in [20]. In this study a trend towards increased vaccine efficacy with increasing age at vaccination was found. According with this study, vaccine efficacy elevated from 85% in children vaccinated at 12 months of age to equal to or more than 94% in those vaccinated at 15 months and older.

#### 1.4 Socio-economic indicators

Pre-primary and primary enrollment rates, urbanization rates and GDPs for the 9 countries considered were taken from [21,22] and used to investigate possible correlations between the estimated country specific transmission rates with illustrative socio-economic indicators that may reflect social mixing patterns characterizing different geographical regions.

Pre-primary and primary enrollment rates range respectively from 1.5% in Ethiopia to 100% in Ireland, and from 37% in Ethiopia to 99% in Republic of Korea. The percentage of individuals living in urban areas ranges from 12% in Ethiopia to 100% in Singapore. Pro-capita GDP ranges from 1,425\$ in Ethiopia to 54,260\$ in United States.

#### 1.3 Model calibration

We firstly calibrate the model defined by the system of ordinary differential equations described above, by considering the transmission rate as the only free model parameter. Consequently, we calibrate the same model, by considering an additional free parameter taking into account the possible uncertainty around the administrative data on coverage levels associated with the Supplementary Immunization Activities performed across different countries. Specifically, in this case, we assume that the coverage level corresponding with a given immunization campaign performed at time  $t$  is  $c_s(t) = x \tilde{c}_s(t)$ , where  $\tilde{c}_s(t)$  is the estimated coverage as reported by administrative records for the SIA considered, and  $0 < x < 1$  is a country-specific free parameter, which is jointly estimated with measles transmission rate.

We compared results obtained with these two alternative model formulations, by using the deviance information criterion (DIC).

The model formulation taking into account an adjusting factor for the reported coverage level associated with SIAs was chosen as it is associated with lower DIC values for all countries where SIAs are performed (see Tab. S4).

Model calibration was carried out separately for each country by performing a Bayesian statistical analysis of published serological data by age.

Since past modeling works have shown that seasonal forcing and time varying recruitment rates (vaccination, birth rates) can lead to chaotic behaviour in the dynamics of infection prevalence, we preferred to keep our calibration procedure

grounded on the more stable epidemiological measure represented by serological profiles [23].

Data used for model calibration were selected from serological prevalence estimates by age available in the literature, using the number of tested and positive individuals among different age segments. When such data were not directly available, these quantities were derived by using the information reported on the overall number of samples, the proportion of samples collected in different age classes, and the percentage of positive samples found at different ages. Moreover, when data were available for both serum and oral fluids tests, data on serum samples were preferred. As a general criterion, as adopted for instance for Singapore, we decided to consider either the earliest or the more detailed age-specific serological profile for our analysis. However, for countries where Supplementary Immunization Activities were performed, multiple serological datasets were used, when possible, to better inform the model on the impact of massive immunization campaigns on the observed changes in the epidemiology of measles. In particular, for UK, since serological datasets were not available after the SIA was performed, the adjusting factor for the reported coverage level of the SIA was fixed to 1. It is important to stress, that even by considering no adjusting in the coverage level characterizing this particular campaign, our estimates suggest that the contribution of the 2013 SIA in UK to the immunity level of individuals at different ages can be considered negligible (see Fig. 4 in the main text).

The sources of data used for model calibration are listed in Tab. S3

COUNTRY	YEAR OF SEROLOGICAL DATA	REFERENCES
<b>CALIBRATION</b>		
Australia	1997	[24]
Australia	1999	[24]
Ethiopia	1997	[7]
Ethiopia	1999	[7]
Ethiopia	2000	[25]
Ireland	1992	[26]
Ireland	2003	[27]
Italy	1978	[28]
Italy	1996	[29]
Italy	2004	[30]
Italy	2006	[31]
Kenya	2001	[32]
Kenya	2002	[32]
Republic of Korea	2001	[33]
Republic of Korea	2002	[34]
Republic of Korea	2010	[34]
Singapore	1993	[35]
UK	2000	[27]
US	1999	[36]

**Tab. S3 Serological data used for model calibration**



Serological studies conducted over time and across countries have used different methods to estimate seroprevalence among individuals of different ages, using alternatively blood or oral fluid samples. Although the threshold chosen to classify individual samples as positive and negative is consistent across the papers, suitable information on equivocal samples is not always available. We therefore decided to rely on the definition of seropositive individuals adopted within the published papers. The free parameters in the selected model are therefore the measles transmission rate  $\beta$  and the coverage adjusting factor for supplementary immunization activities  $x$ . The estimation of the posterior distributions of these two parameters was carried out by means of a Monte Carlo Markov chain (MCMC) approach with random walk Metropolis-Hastings sampling applied to the binomial likelihood of the observed country-specific measles serological profiles [37]. In particular, we assume that the number of immune individuals in each age class is distributed according to a Binomial distribution  $B(n,p)$  and that the likelihood associated with a specific transmission rate and a specific serological profile is:

$$f(\beta, x|n, k) = \prod_{a=1}^{a_M} \binom{n(a)}{k(a)} p(a; \beta, x)^{k(a)} (1 - p(a; \beta, x))^{n(a) - k(a)}$$

where  $a$  runs over the age classes of the country-specific observed serological profile;  $n(a)$  is the number of tested individuals in the age class  $a$ ;  $k(a)$  is the number of positive individuals in age class  $a$ ;  $p(a; \beta, x)$  is the estimated seroprevalence in the year of data collection in age class  $a$  as obtained by model simulation with a specific transmission rate  $\beta$  and coverage adjusting factor  $x$ .

Different chains were initialized with a certain value of  $\beta$  and  $x$ . At each iteration, a log scale was used for sampling, as parameters  $\beta$  and  $x$  are positive definite [38]. In particular, if  $\check{\beta}$  and  $\check{x}$  are the current values and  $z_1, z_2$  are generated from a  $N(0, 1)$ , the new values for these two parameters are defined as  $\beta^* = \check{\beta} e^{\sigma_1 z_1}$  and  $x^* = \check{x} e^{\sigma_2 z_2}$ , and  $\beta^*$  and  $x^*$  are accepted according to the Metropolis Hastings algorithm. The parameters  $\sigma_1$  and  $\sigma_2$  were chosen in order to obtain an acceptance rate of roughly 20-30%. Convergence of MCMC was assessed by considering chains associated with several different starting points, and by visual inspection of 10,000 iterations, after a burn-in period of 2,000 iterations.

In order to obtain independent samples, and avoid auto-correlation among adjacent samples, the chains were thinned, and estimates of the posterior distributions of  $\beta$  and  $x$  were obtained by considering one sample every 25 iterations.

Fig. S9 shows for each country the likelihood variation within the joint posterior distribution of the two model free parameters.

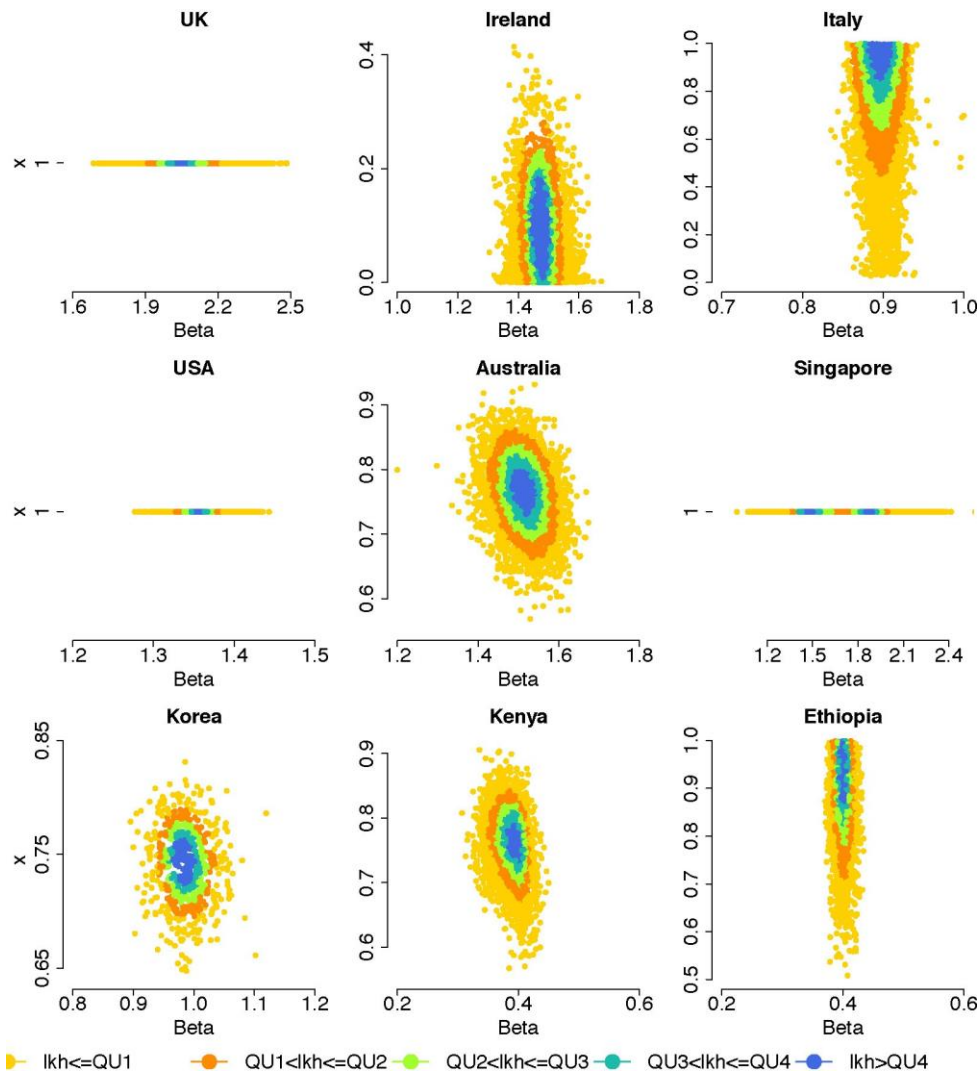


**Fig. S9 Likelihood variability within the joint posterior distribution of the two free model parameters**

The goodness of fit of the model was formally quantified with different indices such as the root mean square error (RMSE) between the observed and predicted percentage of seropositive individuals among different age segments for different countries; the coefficient of determination ( $R^2$ ) and the p-value associated with a Pearson correlation between data points and mean model estimates; the percentage of data points for which the uncertainty surrounding observed seroprevalence values intersect with 95% CI of posterior model estimates; and finally the deviance information criterion (DIC) associated with results obtained through the MCMC procedure. The RMSE is below 8% for all countries except Singapore, showing a very good fit between observed and predicted age specific seroprevalence. In Singapore both the significant positive correlation ( $pvalue < 0.001$ ) found between model estimates and serological prevalence reported in the literature and the percentage of overlapping intervals (60%) show a good fit despite the relatively high value for the RMSE. All the indices are reported in Tab. S4.

Country	Goodness of fit measures				
	Pearson correlation pvalue	% overlapping CI	RMSE	DIC model (p as free parameter)	DIC model (Q and x as free parameter)
Australia	<0.001	87.5	5.4	199	153
Ethiopia	0.0189	72.2	7.4	371	372
Ireland	<0.001	80	6.6	439	348
Italy	<0.001	62.5	7.0	1279	
Kenya	<0.001	100	4.2	209	95
Republic of Korea	<0.0001	72.72	6.3	1360	1014
Singapore	<0.001	60	9.9	187	
UK	<0.001	94.74	1.8	188	
US	0.4603	25	3.5	1130	

Tab. S4 Goodness of fit

The posterior distribution of the parameters  $\beta$  and  $x$  are shown in Fig. S10.

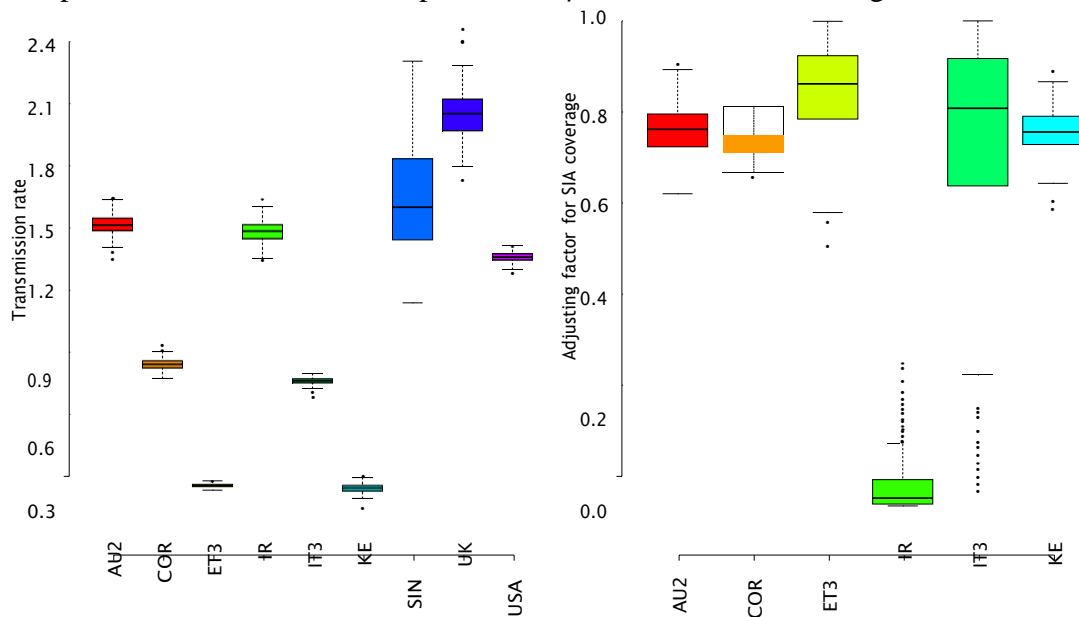
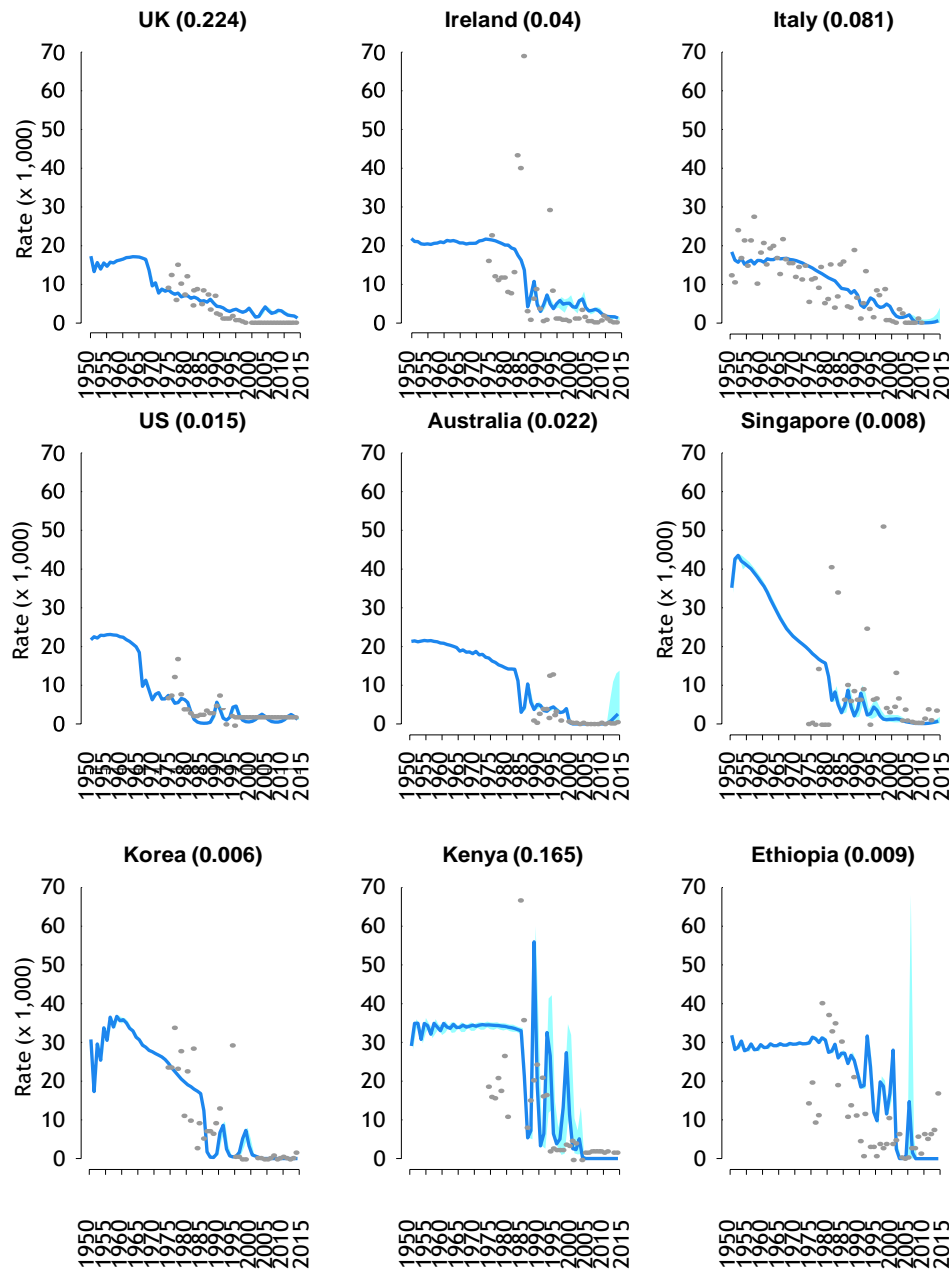


Fig. S10 Posterior distributions of the free parameters

## 1.5 Model validation

The calibrated model was validated against different observed epidemiological data. In particular, we first compare the estimated temporal changes in measles infection rates across the 9 countries considered with the time-series of measles incidence between 1974 and 2015, as provided by WHO records [3] (completed with earlier data available only for Italy [39]). These data usually represent only a fraction of the cases and are available for a period of time that overlaps with epidemiological changes led by vaccination programs, which makes it difficult to robustly assess the impact of demographic changes alone on measles circulation. However, the two

datasets provide useful epidemiological evidences to partially validate the obtained model predictions (see Fig S11). More specifically, we found that the correlation between observed and estimated trends of measles incidence during the last 35 years are significantly positive for all countries, with a coefficient of determination ( $R^2$ ) higher than 85% for 6 out of the 9 countries considered (see Tab. S5).



**Fig. S11** Yearly measles incidence rates per 1,000 individuals as predicted by model simulations (blue lines) and as obtained by adjusting measles cases reported by WHO and the ISS for Italy (grey points) on the basis of a country specific reporting rate. The latter (values shown in brackets) was obtained for each country as the scaling factor minimizing the MSE between model predictions and reported incidence rates

In addition, we investigated the ability of the calibrated model to reproduce the age distribution of cases recorded during recent years in 7 out of the 9 countries under study. The root mean square error (RMSE) between the predicted and observed age distribution of measles cases reported between 2000 and 2015 is lower than 15% for 6 out of 7 considered countries, and lower than 8% for 5 of these. Nonetheless, it is important to stress that measles reported cases represent only a

fraction of the cases and that reporting rates may change with age and across different regions, so that incidence data should be cautiously considered. In particular, data coming from measles outbreaks may provide information on local epidemiological conditions and represent fragmentary evidences on the overall circulation of the infection in the population. This might be for instance the case of records associated with erratic measles cases reported in Korea between 2002 and 2011, as suggested by huge fluctuations in both the number and the age-distribution of measles cases observed during this period (see Fig. S12).

Country	Yearly measles incidence over time		Age distribution of measles cases
	R <sup>2</sup>	Person correlation pvalue	RMSE
Ethiopia	0.929	<0.0001	14.8
Ireland	0.904	<0.0001	6.8
Italy	0.923	<0.0001	3.1; 3.3
Kenya	0.926	<0.0001	6.0
Republic of Korea	0.270	<0.0001	28.1
UK	0.959	<0.0001	6.8
US	0.889	<0.0001	7.2
Australia	0.161	0.014	-
Singapore	0.634	<0.0001	-

Tab. S5 Model validation

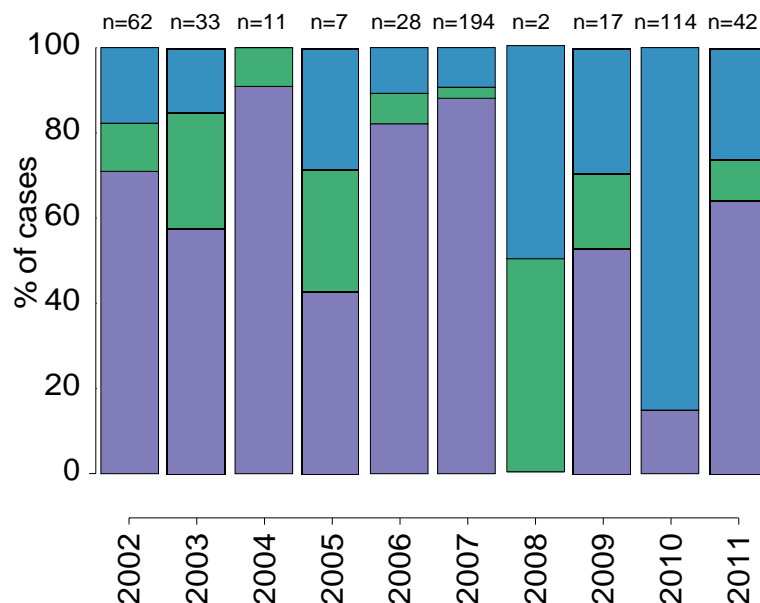


Fig. S12 Age distribution of cases during recent outbreaks in Korea between 2002 and 2011 (0-4y in purple, 5-14y in green and 15-85y in blue). The total number of cases over the years is reported above the bars.

## 1.6 Sensitivity analysis

The assumption of a constant transmission rate over time represents a critical

limitation of the proposed investigation. A sensitivity analysis was therefore carried out in order to assess whether the predicted temporal trends in yearly incidence rates or the estimates obtained for the age specific serological profiles associated with 2015 are affected by the explicit inclusion of seasonal variations in measles transmission caused by school terms. Although detailed time-series of measles incidence in the pre-vaccination era are not available for most of the countries, we use available data on monthly incidence of measles as recorded for the period 1950-1967 in the UK [40], to check for possible effects led by measles seasonality on our epidemiological results.

Specifically, we assume that the measles transmission rate is the product of a constant rate  $\tilde{\beta}$  and a piecewise constant function of the day of the year  $\sigma(\text{day})$ , accounting for possible variation in the transmission of the virus led by the school calendar.

Specifically, we assume that  $\sigma(\text{day})$  is the same for every year considered and that it varies within each year as follows:

$$\sigma(\text{day}) = \begin{cases} 1 - w & \text{if } \text{day} \leq 4 \text{ or } 200 < \text{day} \leq 247 \text{ or } 358 < \text{day} \leq 365 \\ 1 + w & \text{otherwise} \end{cases}$$

where  $w$  drives possible differences in measles transmission between holidays and school term periods.

We calibrated the model with seasonal forcing by fitting monthly temporal series of measles incidence in UK from January 1950 to December 1967. In principle, the model accounting for a seasonal forcing in measles transmission has three degrees of freedom represented by  $\tilde{\beta}$ ,  $w$  and an additional parameter  $\rho$  defining the measles reporting rate. However, it is not possible to univocally determine both the transmission rate and the reporting rate. As a consequence, following a similar approach already used in [41], we forced the model accounting for seasonality to have the same  $R_0$  as the model used in our baseline formulation, therefore fixing  $\tilde{\beta}$  in such a way that the average transmission rate during the year is the one already estimated with a constant transmission. The model accounting for a seasonal variation in measles transmission as driven by school terms has been therefore calibrated by considering two unknown parameters, namely  $w$  and  $\rho$ , which were univocally estimated by maximum likelihood.

For the case of UK and the time period considered, we estimated  $w = 0.52$  and  $\rho = 47\%$ . Panel A in Fig. S13 shows that the model with seasonal forcing is able to capture the observed seasonal pattern in the incidence rates between 1950 and 1967 and to well reproduce the serological profile associated with 2000 in the UK.

Specifically, the yearly peak is perfectly aligned in almost all seasons while the effect of Christmas holidays is always visible in both the predicted and observed incidence over time. The predicted incidence is in excellent agreement with the data ( $R^2 = 0.72$ , p-value  $< 0.0001$ ).

The carried out analysis based on UK measles data confirms recent modeling results obtained for Italy [41], and shows that neither the predicted yearly incidence rates (Fig. S13D,  $R^2 = 0.94$ , p-value  $< 0.0001$ ) in the population nor the estimated longitudinal transition characterizing the immunity profiles of the population over time (Fig. 13B and Fig. 13C) are affected by the simplifying assumption of a constant transmission over the year. In particular, estimates obtained for the serological status of individuals at different age for the population of the UK in 2015 do not differ from estimates obtained for this country when the measles circulation is assumed to be constant within the year, i.e. when no seasonal forcing in the transmission rate is considered.

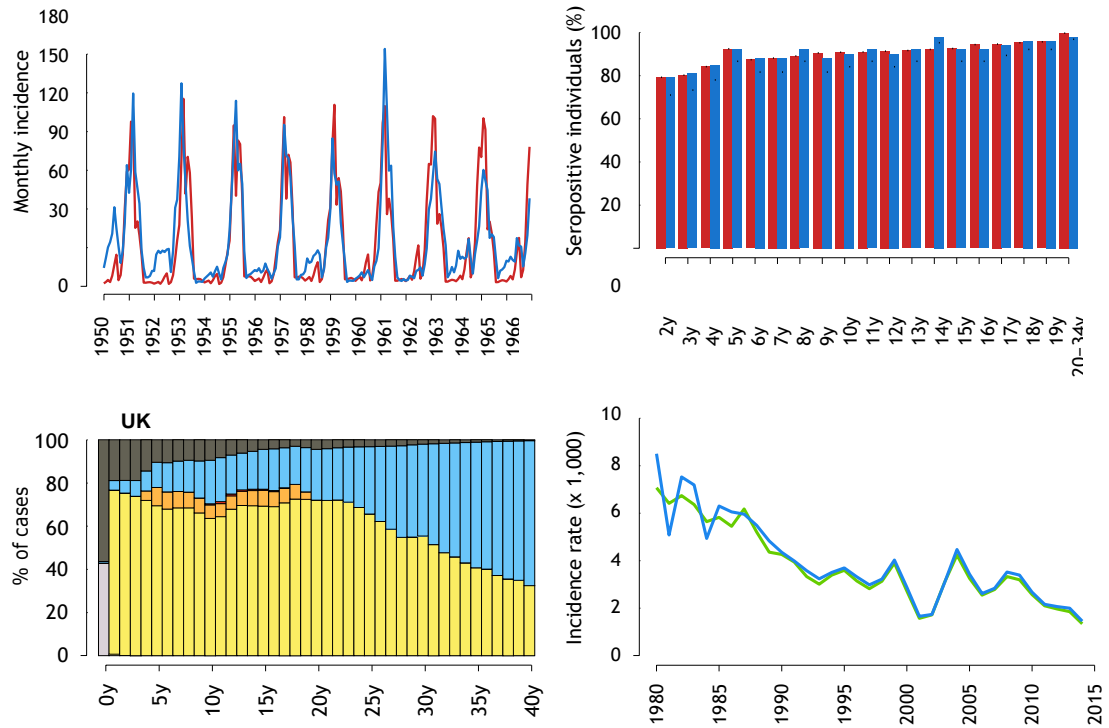


**Fig. S13** A) Monthly incidence over time as reported in UK to the notification systems [40] (blue) and as predicted by the model when assuming a school-driven seasonal variation in the transmission rate and one single reporting rate over time (red). B) Age specific seroprevalence as observed (blue) and as predicted (red) by the model explicitly accounting for the seasonality in measles circulation. C) Model predictions on the epidemiological status at different ages in UK for 2015, as predicted by explicitly accounting for a seasonal forcing in measles circulation. For each age strata it is shown the percentage of individuals susceptible to infection (dark grey), protected against infection by immunity provided by maternal antibodies (light grey), and acquired through natural infection (cyan), routine first dose vaccination (yellow), second booster administration (orange) and SIAs (red). D) Average yearly measles incidence rates per 1,000 over time as predicted by the model explicitly accounting for a seasonal variation in measles transmission driven by school terms (blue) and by assuming a constant measles transmission rate during the year (green).

## 2. Additional results

### 2.1 Measles transmission and socio-economic indicators

Epidemiological differences across countries may rise as a consequence of country specific estimates of measles transmission rate. This result suggests that, beyond local demographic conditions, differences in individuals' social behavior across different geographical area may also reflect the socio-economic status of the population considered. In particular, we performed a simple correlation analysis where the Pearson correlation between the obtained posterior mean of the transmission rate and country-specific socio-economic indicators is computed, and the hypothesis of positive correlation tested through a t-test. A significant positive correlation ( $p < 0.05$ ) was found between country specific transmission rates and their GDP, pre-primary and primary enrollment rates and urbanization rates (Fig. S14. Pearson correlation: 0.76,  $p = 0.005$ ; 0.56,  $p = 0.044$ ; 0.66,  $p = 0.018$ ; 0.85,  $p < 0.001$ ; respectively). Significant correlations ( $p < 0.1$ ) also emerged when Spearman-ranking correlation indices were considered, with the exception of primary enrollment (Spearman-rank correlation: 0.50,  $p = 0.07$ ; 0.52,  $p = 0.06$ ; 0.43,  $p = 0.109$ ; 0.83,  $p = 0.003$ ; respectively).

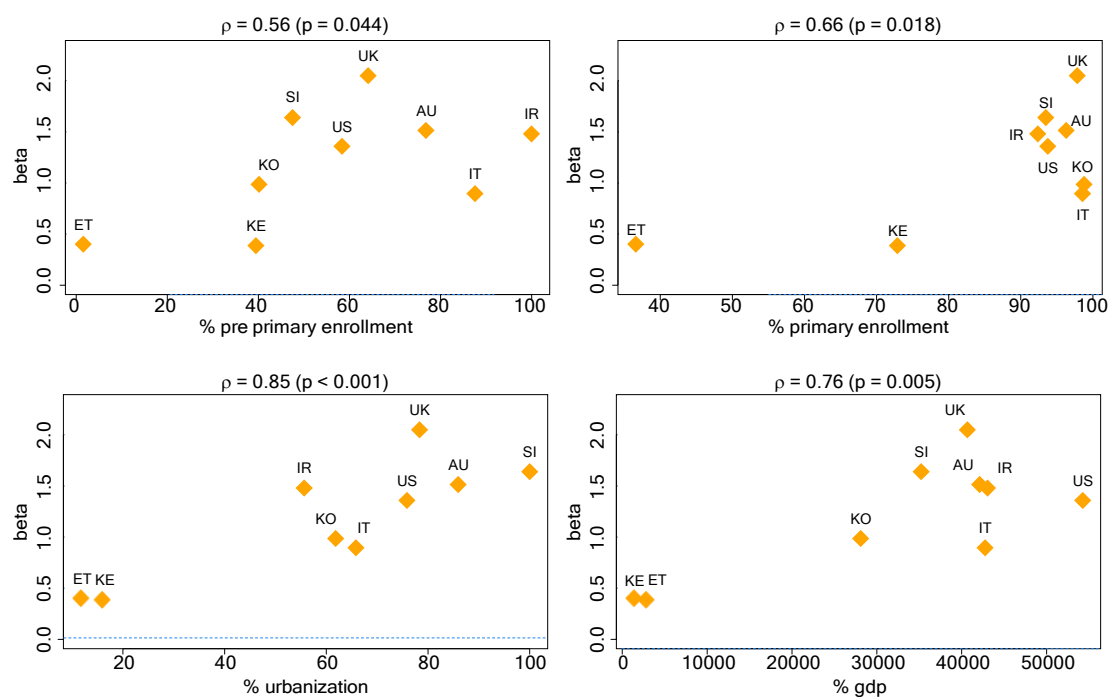


**Fig. S14 Pearson correlations between country specific transmission rates and illustrative socio economic indicators.**

### 2.2 Measles transmissibility potential

Measles transmissibility potential can be quantified by the basic reproduction number ( $R_0$ ), representing the average number of secondary infections generated by a typical index case in a fully susceptible population during the entire period of infectiousness. In particular, if  $R_0$  is greater than 1 the infection spreads in the population generating a major epidemic and may lead to endemic persistence of the infection; if  $R_0$  is smaller than 1 the infection will die out, after the generation of sporadic infection events.



The basic reproduction number can be computed as the dominant eigenvalue  $\rho$  of the next generation matrix (NGM) associated with the transmission model considered [42].

Following the approach proposed in [41], it can be shown that changes in the crude birth rate from  $b$  to  $b^*$  are mathematically equivalent to a change in the transmission rate from  $\beta$  to  $\beta^* = \beta \frac{b^*}{b}$ . As a consequence, measles transmissibility potential is expected to change over time and the NGM associated with years  $y \in \{1951, \dots, 2015\}$  can be computed as follows:

$$nGM(y) = \beta \frac{b(y)}{\hat{b}} \begin{pmatrix} \frac{x(0, y)}{! + d(0, t)} & \cdots & \frac{x(0, y)}{! + d(85, t)} \\ \vdots & \vdots & \vdots \\ \frac{x(85, y)}{! + d(0, t)} & \cdots & \frac{x(85, y)}{! + d(85, t)} \end{pmatrix}$$

where  $x(a, y)$  represents the fraction of individuals of age  $a$  in the population of year  $y$ , and  $\hat{b}$  is the birth rate used to obtain the epidemiological equilibrium associated with constant fertility and mortality rates fixed to values observed in 1950.

The fraction of immunized individuals required at a population level for measles elimination it is therefore estimated to change over time and can be computed as

$$p(y) = \left(1 - \frac{1}{\rho^{nGM(y)}}\right)$$

where  $\rho^{nGM(y)}$  is the dominant eigenvalue associated to the next generation matrix  $nGM(y)$ . Variations over time in such a threshold value are shown for five illustrative countries in Fig. S15 (left panel).

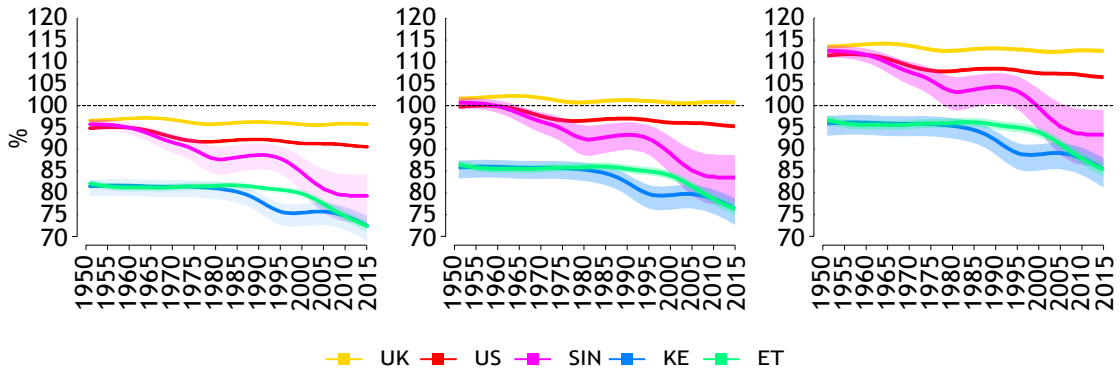


**Fig. S15** Estimated percentage of immunized individuals required at a population level at different years to achieve measles elimination among 5 illustrative countries, when vaccine efficacy is assumed to be 100% (left), 95% (center) and 85% (right). Central model estimates are shown as bold lines, while shaded areas represents 95% CI associated with obtained estimates.

In the left panel of Fig. S15 we show the percentage of the overall population that should be successfully immunized in order to locally eliminate the infection, therefore representing the illustrative - but also unrealistic - case of a perfect vaccination (i.e. 100% vaccine efficacy). However, the percentage of individuals that should be vaccinated can remarkably increase when the vaccine efficacy is assumed to be either 85% or 95%, depending on age at vaccine administration. As a consequence, when the effective coverage level required for measles elimination is estimated to be 90% but the vaccine is administered at 9 months (so that the vaccine efficacy is 85%),

even a 100% of vaccine uptake would be inadequate to eliminate the disease, so that the administration of multiple vaccine doses would be required to attain a sufficiently high fraction of successfully immunized individuals in the population. Central and right panels of Fig. S15 show the proportion of effectively immunized individuals that is required at a population level (i.e. among all ages) to achieve local measles elimination under different assumption on the vaccine efficacy.

### 2.3 Measles transmission and fertility trends

Let us consider a simple SIR model accounting for the vital dynamics of the population as defined by the following ordinary differential equations:

$$\begin{cases} \dot{S} = bn - \beta S \frac{I}{n} - dS \\ \dot{I} = \beta S \frac{I}{n} - (\gamma + d)I \\ \dot{R} = \gamma I - dR \end{cases} \quad (1)$$

where  $b$  and  $d$  are the birth and death rates respectively, and are assumed to be constant over time. The dynamics of the total population  $n(t) = S(t) + I(t) + R(t)$  is defined by the following equation:

$$\dot{n} = (b - d)n$$

and therefore the total population  $N(t)$  evolves exponentially over time as follows:

$$n(t) = n_0 e^{(b-d)t}.$$

The qualitative dynamics of this system can be investigated analytically. Specifically, by introducing the epidemiological fractions  $x = \frac{S}{n}$  and  $y = \frac{I}{n}$ , the system (1) becomes:

$$\begin{cases} \dot{x}(t) = b(1 - x(t)) - \beta x(t)y(t) \\ \dot{y}(t) = \beta x(t)y(t) - (b + \gamma)y(t) \end{cases}$$

It can be easily shown that when  $\beta > b + \gamma$ , the system admits the following unique endemic steady state:

$$x^* = \frac{b + \gamma}{\beta} \quad y^* = \frac{b}{b + \gamma} \left(1 - \frac{b + \gamma}{\beta}\right)$$

and that the force of infection at the endemic equilibrium is defined by the following equation.

$$\lambda^* = \beta y^* = \beta \frac{b}{b + \gamma} \left(1 - \frac{b + \gamma}{\beta}\right)$$

Since the birth rate  $b$  is much smaller than measles recovery rate  $\gamma$ , we can approximate  $b + \gamma \approx \gamma$ , therefore obtaining:

$$y^* = \frac{b}{\gamma} \left(1 - \frac{\gamma}{\beta}\right) \quad \lambda^* = b \frac{\beta}{\gamma} \left(1 - \frac{\gamma}{\beta}\right)$$

This two equilibrium values show both the infection incidence ( $y^*$ ) and the force of infection ( $\lambda^*$ ) increase with the birth rate.

The effective reproduction number  $R_{eff}$  is defined by the number of secondary infections generated by a single infected individual during her/his infectious period in a partially immunized population. The dynamics over time of the effective reproductive number can be simulated by computing at each time step the amount of susceptible individuals in the overall population and by estimating the number of secondary infections generated by a single infectious cases as

$$R_{eff}(t) = \frac{\beta \sum_{a=0}^{85} S(a, t)}{\sum_{a=0}^{85} n(a, t)}$$

Moreover, the contribution of population age segments in sustaining the infection transmission among susceptible individuals can be quantified by computing the expected number of secondary infections generated among different age classes ( $a1, a2$ ) according to the following equation:

$$R_{eff}(a1, a2; t) = \frac{\beta \sum_{a=a1}^{a2} S(a, t)}{\sum_{a=a1}^{a2} n(a, t)}$$

The temporal dynamics of  $R_{eff}$  and the contribution of young children, adolescents and adults in sustaining the measles transmissibility are shown in Fig. S16.

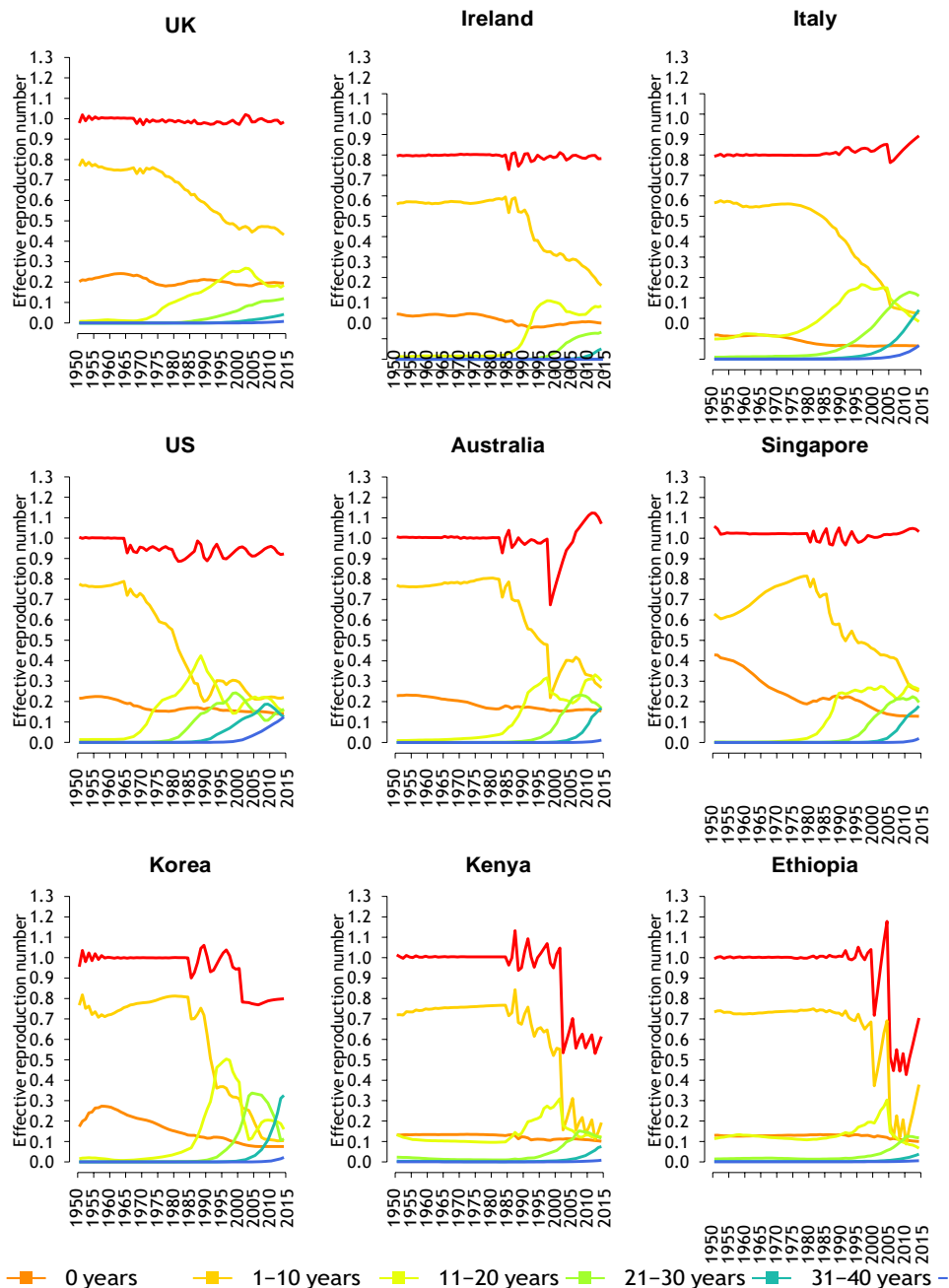


**Fig. S16** The dynamics of the effective reproduction number among different countries (red line) and the contribution of susceptible individuals of different age segments in sustaining measles transmission.

Interestingly, a positive Spearman-ranking correlation ( $p$ -value $<0.05$ ) is found between the fraction of the population older than 50 years of age and the value of the estimated effective reproduction number in 2015.

It is important to stress that the predicted temporal trends for the effective reproductive number are based on the two strong assumptions of homogeneous mixing and constant measles transmission rate over time. As a consequence, these results should be considered only as illustrative of changes in measles epidemiology caused by time-varying basic demographic components.

Fig. S17 shows a comparison between observed temporal changes in measles circulation in Italy and the corresponding trends in birth rates associated with this country, since data are available for a longer period of time (since 1926). We found that measles incidence rates recorded before the start of vaccination are strongly correlated with the reported crude birth rates ( $\rho = 0.68$ ,  $p$ -value  $< 0.01$  without moving average, and  $\rho = 0.87$ ,  $p$ -value  $< 0.01$  if averaged over a moving window of 7

years) suggesting a strong relation between infection and fertility trends over time. This analysis provides an empirical evidence supporting the predicted impact of demographic changes on measles circulation.

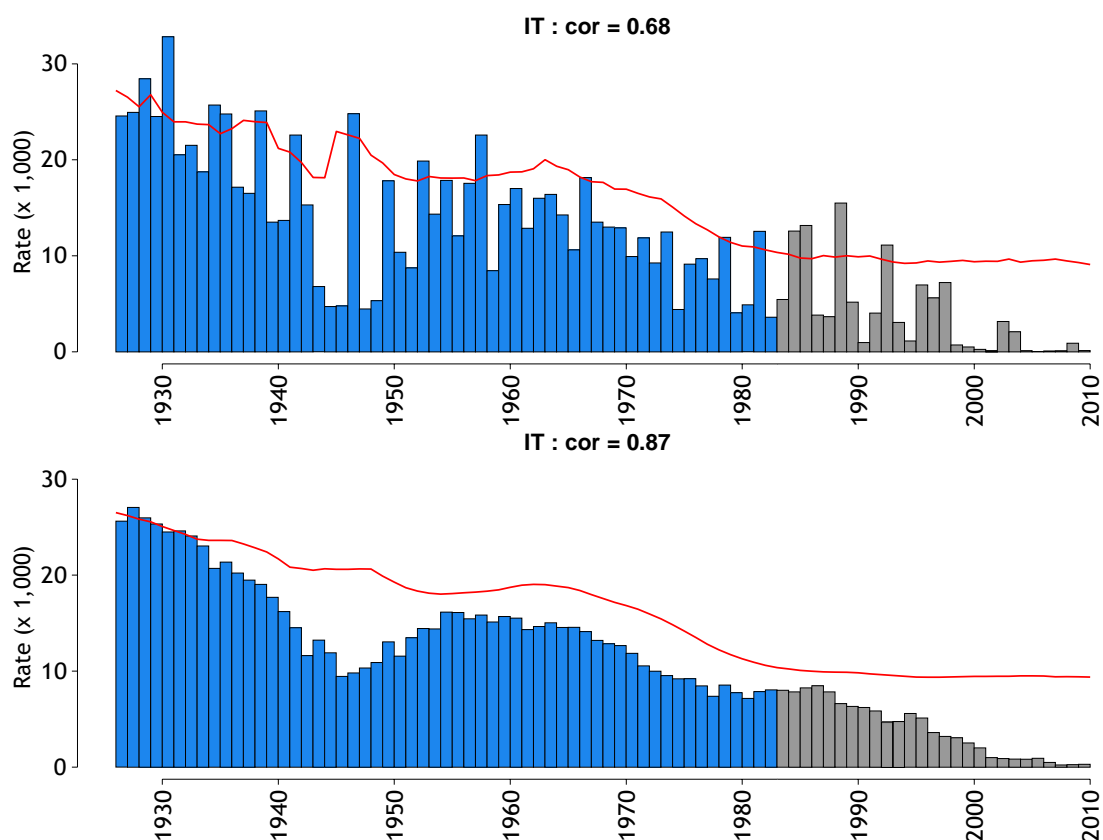
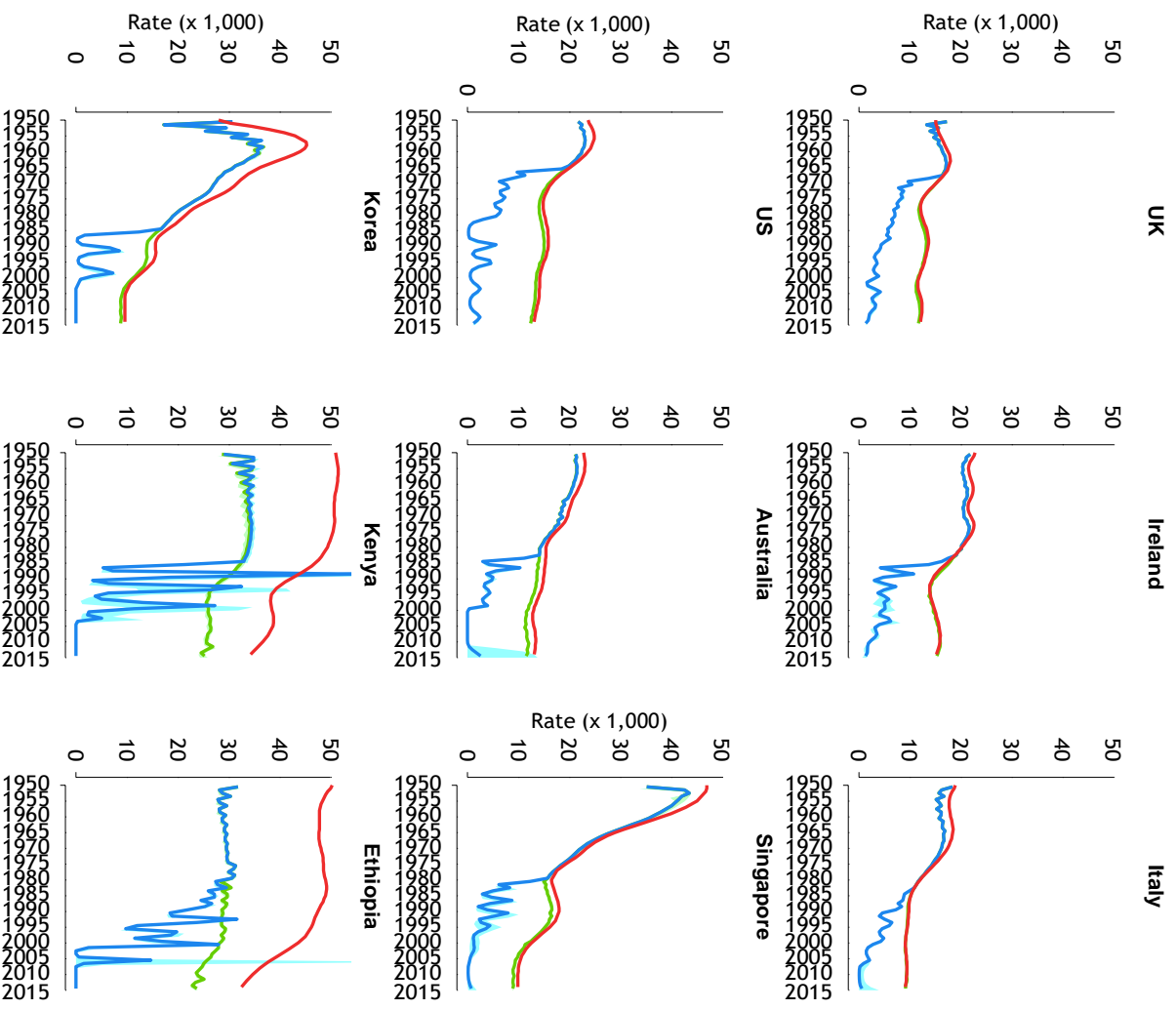


**Fig. S17** Top panel shows the observed measles incidence as reported to the Italian statutory notification system before (blue) and after (grey) the introduction of first dose vaccination, and temporal changes in the crude birth rate as occurred between 1950 and 2010 (red line). Bottom panel below shows the same quantity averaged over a moving window of 7 years.

## 2.4 Temporal changes in measles epidemiology

In order to disentangle the contribution of local demographic conditions and country specific vaccination strategies in shaping measles epidemiology among different countries, two different scenarios were considered. The first one simulates the natural history of the infection in the absence of vaccination and aims at highlighting the impact of demographic processes on the measles transmission dynamics. The second one, include both demographic changes and immunization activities performed during the last 35 years.

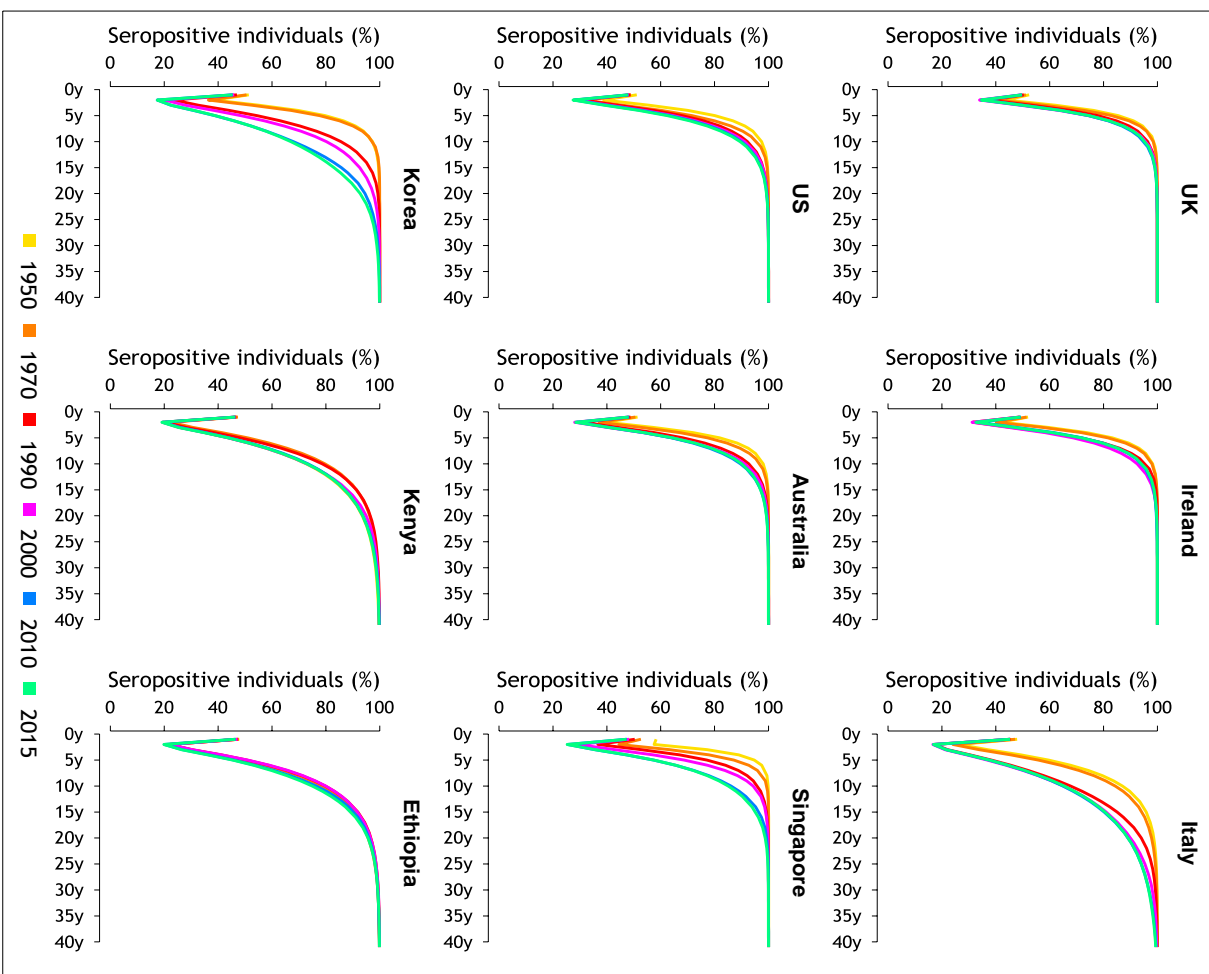
Obtained estimates associated with the two different scenarios for each country considered are summarized by Fig. S18. In particular, the dynamics of measles incidence over time is shown along with the crude birth rate.



**Fig. S18** Reported crude birth rate (red line) and estimated incidence rates over time in the absence of vaccination (green line) and as obtained by mimicking country specific immunization activities (blue line).

The expected evolution of age specific serological profile over time associated with the two different scenarios is shown in Fig. S19 and S20.

Fig. S19 Estimated evolution of age specific serological profiles in the absence of vaccination.



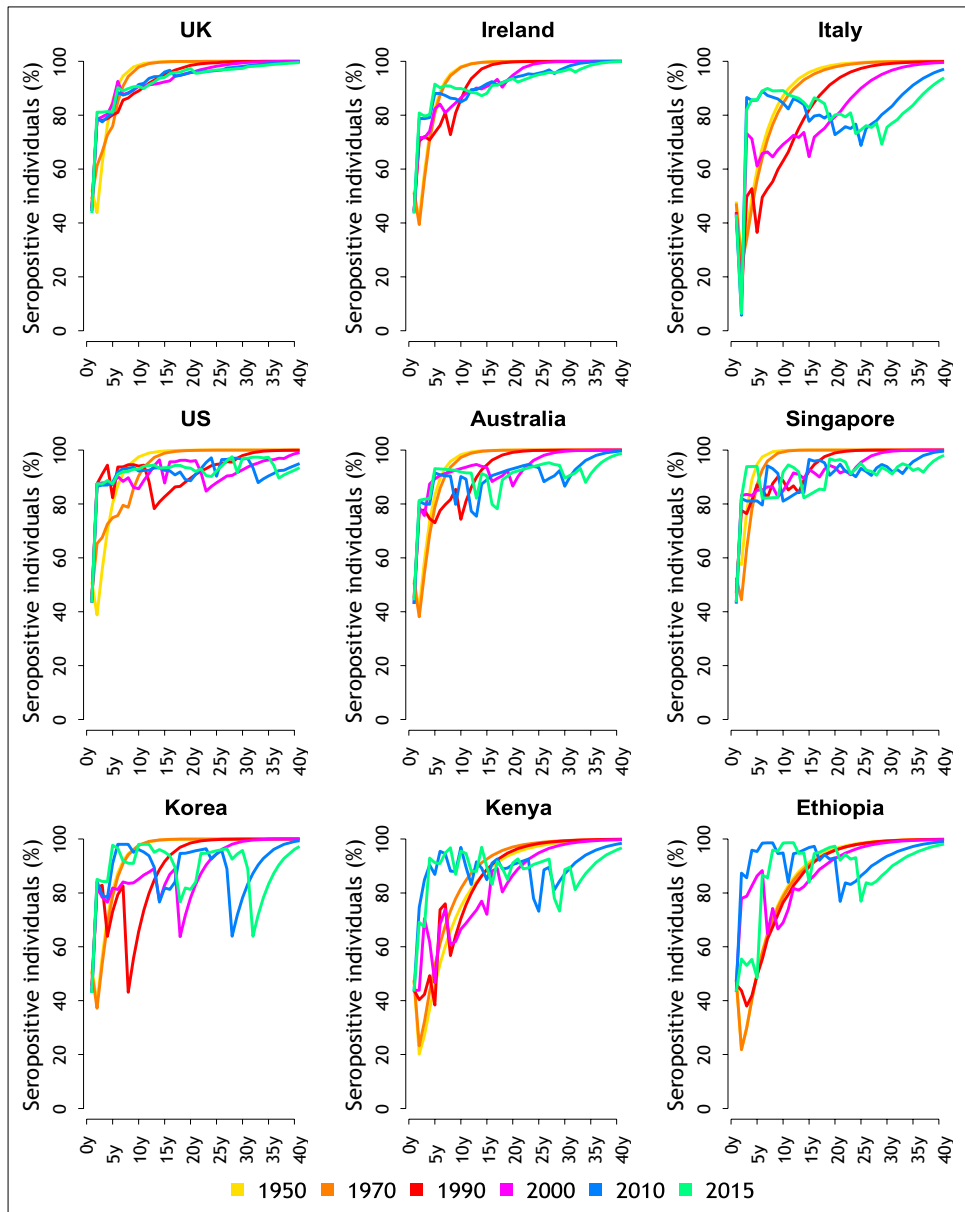


**Fig. S20 Evolution of age specific serological profiles as obtained by mimicking country specific immunization activities performed during the period 1950-2015.**

Finally the expected evolution of median age at infection over time associated with the two different scenarios is shown in Fig. S21. For example in Italy, in the absence of vaccination, the median age at infection in 2015 is estimated between 5 and 6 years of age; when all vaccination strategies are considered, the median age at infection in 2015 raises to 20 years of age. This estimate is compliant with evidences recently reported by the Istituto Superiore di Sanità [39].



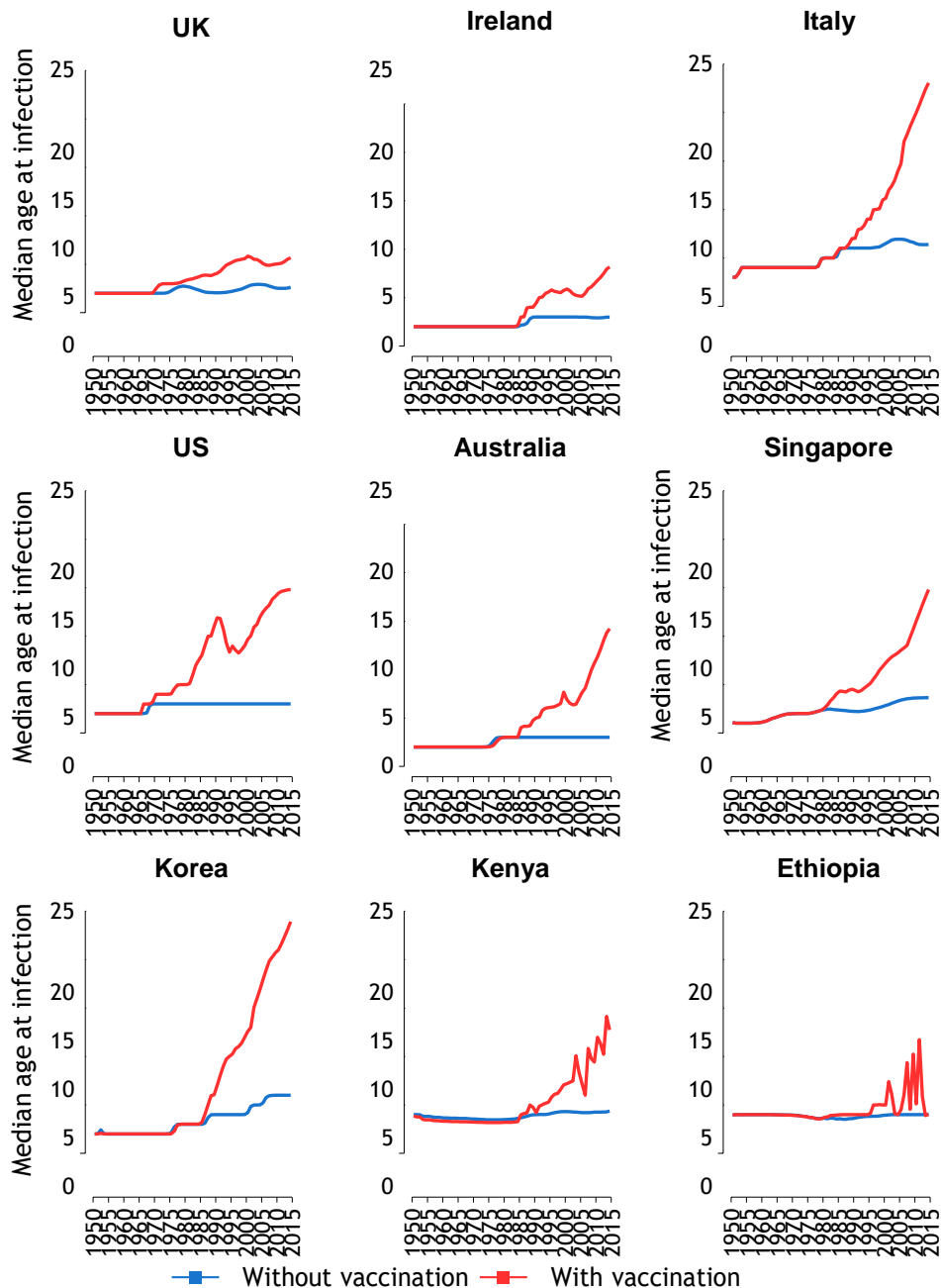


**Fig. S21 Evolution of median age at infection as obtained in absence of vaccination and by mimicking country specific immunization activities performed during the period 1950-2015.**

## 2.5 Within country heterogeneity in measles epidemiology: the case of Ethiopia

Most of results discussed in the main text are based on the simplistic assumption of homogeneous coverage levels within countries. Possible heterogeneities in measles epidemiology rising from different vaccine uptake among different regions of the same country are highlighted by simulating two illustrative scenarios based on available data on coverage levels in different regions of Ethiopia [8]. These data were specifically used to compare the epidemiological status estimated in 2015 associated with low-coverage and high-coverage regions. The results are summarized in Fig. S22, where the percentage of susceptible and immune individuals are highlighted at different ages. Similarly to results presented in the main text, immune individuals are further stratified in those who acquired immunity from natural infection and in those vaccinated during different immunization activities.

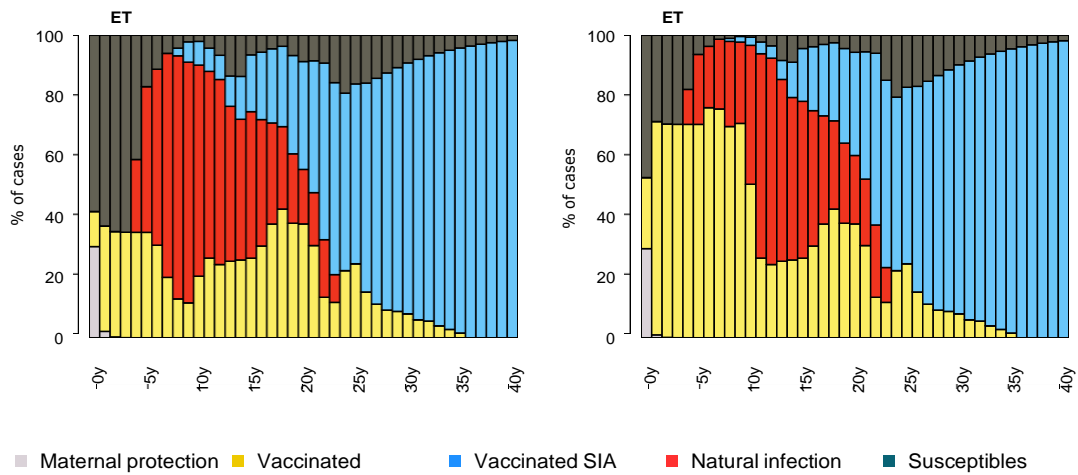


**Fig. S22 Epidemiological status estimated for different ages in low coverage areas (a) and high coverage areas (b) of Ethiopia, based on regional records reported in [8].**

## 2.6 Current epidemiology of measles among different countries

Model estimates on the distribution of the residual susceptibility among different age classes in the 9 countries considered are shown in Fig. S23.

Fig. S24 shows the estimated percentage of susceptible (a) and naturally infected (b) individuals in the overall population, and the percentage of successfully immunized individuals that can be ascribed to different vaccination activities performed in different countries (c).

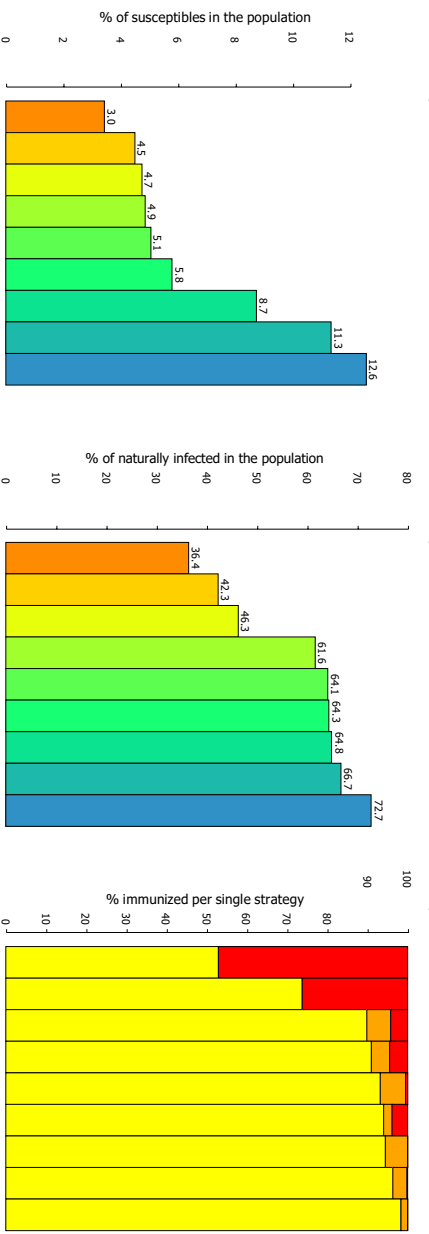
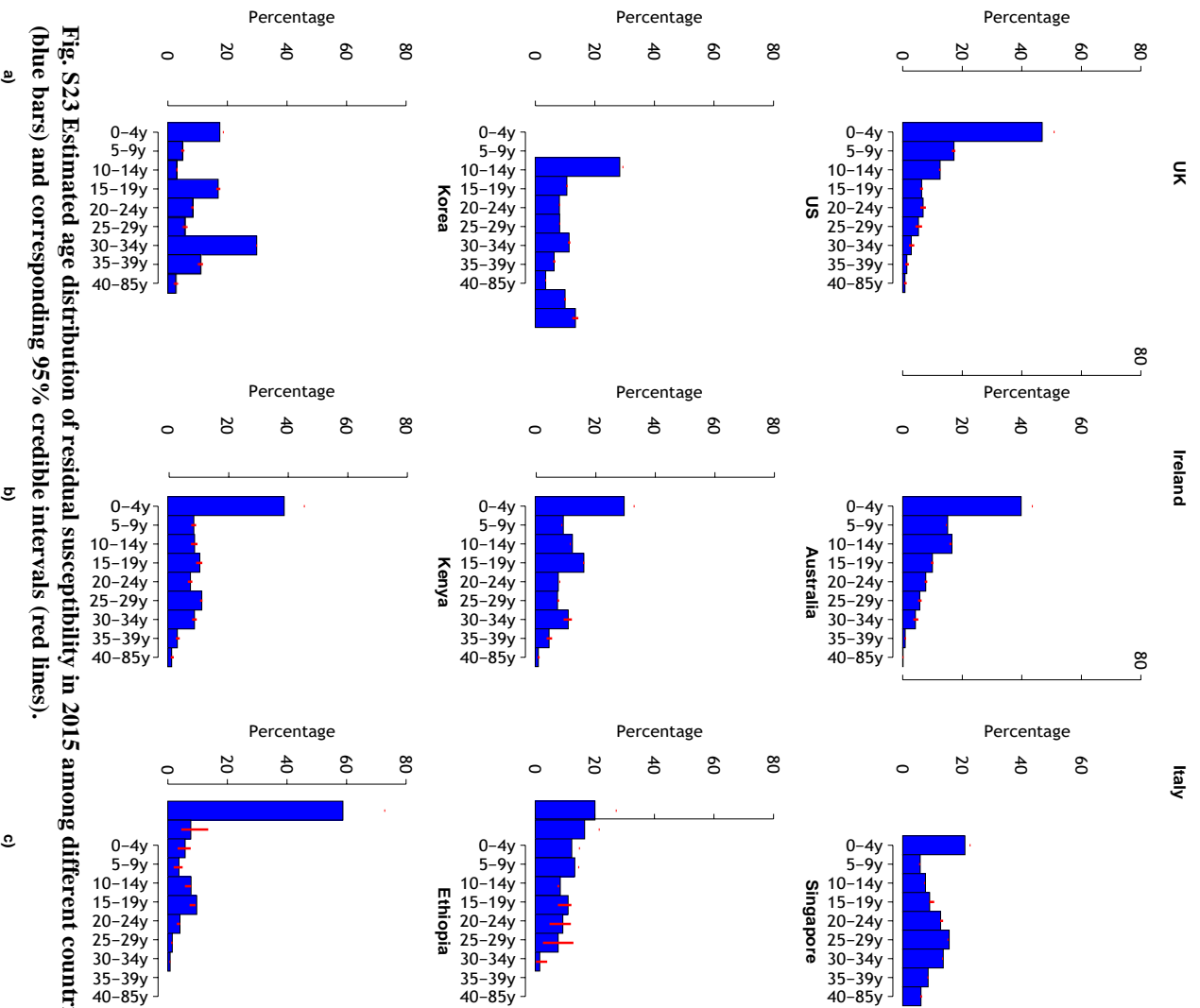


**Fig. S24 a)** Estimated percentage of susceptible individuals in the host population in 2015. b) Percentage of the host population protected in 2015 as a consequence of past measles infection. c)

**Percentage of successfully immunized individuals ascribable to first dose (yellow), second booster (orange) and SIA (red).**

Finally we estimated through model simulation the temporal changes in the proportion of immune individuals in the population between 1950 and 2015 across different countries, highlighting the progressive replacement of naturally acquired immunity with immunity caused by vaccination (Fig. S25). The obtained estimates highlight the potential risks represented by 1) a decline of future routine coverage levels, especially for countries where 1<sup>st</sup> dose routine programs have reached a high uptake level early in the 80s, such as in US, and 2) the interruption of frequent catch-up campaigns in those countries where routine coverage are still critically low. The latter is the case of Kenya and Ethiopia, where low routine vaccine uptake are exacerbated by the 85% of vaccine efficacy associated with vaccine administration at 9 months.

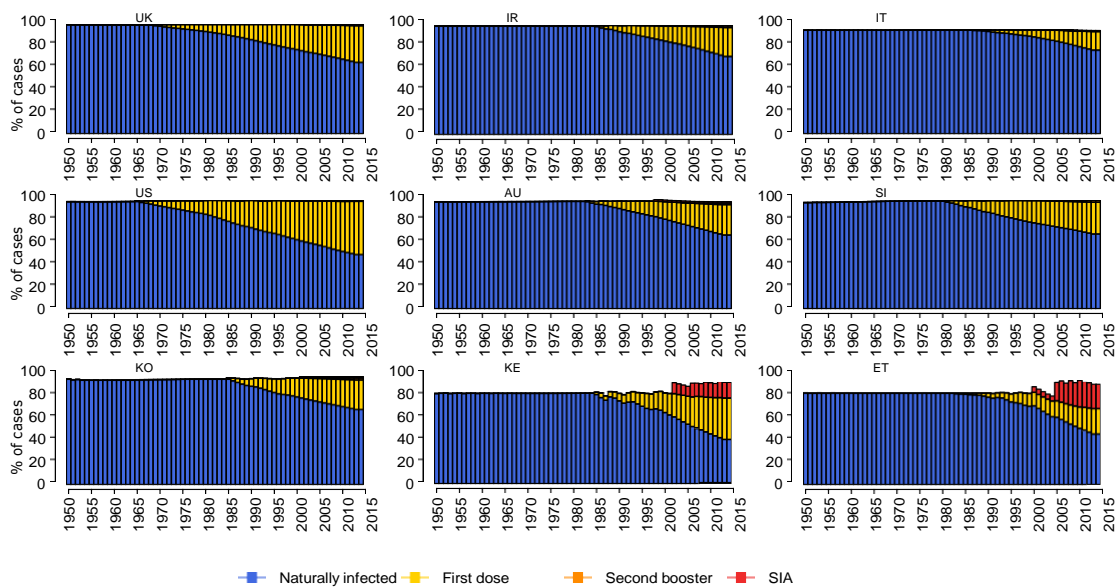


**Fig. S25 Estimated percentage of successfully immunized individuals in the host population ascribable to first dose (yellow), second booster (orange), SIA (red), and natural infection (blue) in the period 1950-2015**

## References

1. <http://esa.un.org/unpd/wpp/DataQuery/>
2. <http://esa.un.org/MigGMGProfiles/indicators/indicators.htm>
3. [http://www.who.int/immunization/monitoring\\_surveillance/data/en/](http://www.who.int/immunization/monitoring_surveillance/data/en/)
4. <http://www.salute.gov.it>
5. Hinman, A. R., Kolasa, M. S., Klemperer-Johnson, S., Papania, M. J. (2004). Progress toward implementation of a second-dose measles immunization requirement for all schoolchildren in the United States. *Journal of Infectious Diseases*, 189(Supplement 1), S98-S103
6. Turnbull, F. et al (2001). The Australian measles control campaign, 1998. *Bulletin of the World Health Organization*, 79(9), 882-888
7. Nigatu, W. et al (2008). Evaluation of a measles vaccine campaign in Ethiopia using oral-fluid antibody surveys. *Vaccine*, 26(37), 4769-4774
8. Mitiku, K. et al (2011). Progress in measles mortality reduction in Ethiopia, 2002–2009. *Journal of Infectious Diseases*, 204(suppl 1), S232-S238
9. Gee, S., Cotter, S., & O'Flanagan, D. (2010). Spotlight on measles 2010: measles outbreak in Ireland 2009-2010. *Euro surveillance: bulletin européen sur les maladies transmissibles*
10. Khetsuriani, N. et al (2011). Supplementary immunization activities to achieve measles elimination: experience of the European Region. *Journal of Infectious Diseases*, 204(suppl 1), S343-S352.
11. <http://www.lenus.ie/>
12. <http://circulars.gov.ie/>
13. Bonanni, P. et al (2007). Progress in Italy in control and elimination of measles and congenital rubella. *Vaccine*, 25(16), 3105-3110
14. <http://www.cdc.gov/mmwr/preview/mmwrhtml/mm5637a5.htm>
15. <http://www.cdc.gov/mmwr/preview/mmwrhtml/mm6134a4.htm>
16. <http://www.cdc.gov/mmwr/preview/mmwrhtml/mm6313a3.htm>
17. Choe, Y. J., Jee, Y., Oh, M. D., Lee, J. K. (2015). Measles elimination activities in the Western Pacific Region: experience from the Republic of Korea. *Journal of Korean medical science*, 30(Suppl 2), S115-S121
18. Simone, B. et al (2014). Evaluation of the measles, mumps and rubella vaccination catch-up campaign in England in 2013. *Vaccine*, 32(36), 4681-4688.
19. Allam, M. F. (2009). Measles vaccination. *Journal of Preventive Medicine and Hygiene*, 50, 201-205
20. De Serres G., Boulianne N., Meyer F., Ward B. (1995). Measles vaccine efficacy during an outbreak in a highly vaccinated population: incremental increase in protection with age at vaccination up to 18 months. *Epidemiology and infection*, 115(02), 315–323.
21. <http://www.worldbank.org/>
22. <http://www.oecd.org/>

23. Earn, D. J., Rohani, P., Bolker, B. M., Grenfell, B. T. (2000). A simple model for complex dynamical transitions in epidemics. *Science*, 287(5453), 667-670
24. Gilbert, G. L. et al (2001). Impact of the Australian Measles Control Campaign on immunity to measles and rubella. *Epidemiology and infection*, 127(02), 297-303.
25. Nokes, D. J. et al (2001). Has oral fluid the potential to replace serum for the evaluation of population immunity levels?: a study of measles, rubella and hepatitis B in rural Ethiopia. *Bulletin of the World Health Organization*, 79(7), 588-595
26. Johnson, H., Hillary, I. B., McQuoid, G., Gilmer, B. A. (1995). MMR vaccination, measles epidemiology and sero-surveillance in the Republic of Ireland. *Vaccine*, 13(6), 533-537
27. Andrews, N. et al (2008). Towards elimination: measles susceptibility in Australia and 17 European countries. *Bulletin of the World Health Organization*, 86(3), 197-204
28. Santoro, R., (1984). Measles epidemiology in Italy. *International journal of epidemiology*, 13(2), 201-209
29. Salmaso, S. et al (2000). Pattern of susceptibility to measles in Italy. *Bulletin of the World Health Organization*, 78(8), 950-955
30. Rota, M. C. et al (2008). Measles serological survey in the Italian population: interpretation of results using mixture model. *Vaccine*, 26(34), 4403-4409
31. Bechini, A. et al (2012). Progress towards measles and rubella elimination in Tuscany, Italy: the role of population seroepidemiological profile. *The European Journal of Public Health*, 22(1), 133-139
32. Ohuma, E. et al (2009). Evaluation of a measles vaccine campaign by oral-fluid surveys in a rural Kenyan district: interpretation of antibody prevalence data using mixture models. *Epidemiology and infection*, 137(02), 227-233
33. Kim, S. S., Han, H. W., Go, U., Chung, H. W. (2004). Sero-epidemiology of measles and mumps in Korea: impact of the catch-up campaign on measles immunity. *Vaccine*, 23(3), 290-297
34. Choe, Y. J., Bae, G. R. (2012). Current status of measles in the Republic of Korea: an overview of case-based and seroepidemiological surveillance scheme. *Korean journal of pediatrics*, 55(12), 455-461
35. Ho, H. J. et al (2014). Progress towards measles elimination in Singapore. *Vaccine*, 32(51), 6927-6933
36. McQuillan, G. M. et al (2007). Seroprevalence of measles antibody in the US population, 1999–2004. *Journal of Infectious Diseases*, 196(10), 1459-1464
37. Cauchemez, S., Carrat, F., Viboud, C., Valleron, A. J., Boelle, P. Y. (2004). A Bayesian MCMC approach to study transmission of influenza: application to household longitudinal data. *Statistics in medicine*, 23(22), 3469-3487
38. Dorigatti, I., Cauchemez, S., Pugliese, A., Ferguson, N. M. (2012). A new approach to characterising infectious disease transmission dynamics from sentinel surveillance: application to the Italian 2009–2010 A/H1N1 influenza pandemic. *Epidemics*, 4(1), 9-21
39. <http://www.epicentro.iss.it/focus/morbillo/morbillo.asp>
40. <https://ms.mcmaster.ca/~bolker/measdata.html>
41. Merler, S., Ajelli, M. (2014). Deciphering the relative weights of demographic transition and vaccination in the decrease of measles incidence in Italy. *Proceedings of the Royal Society of London B: Biological Sciences*, 281(1777), 20132676

42. Diekmann, O., Heesterbeek, J. A. P., Metz, J. A. (1990). On the definition and the computation of the basic reproduction ratio  $R_0$  in models for infectious diseases in heterogeneous populations. *Journal of mathematical biology*, 28(4), 365-382.